INVITED PAPER

Optical Switching in Future Fiber-Optic Networks Utilizing Spectral and Spatial Degrees of Freedom

This article examines the capacity scaling requirements of optical networks from a switching perspective that leverage both spectral and spatial degrees of freedom.

By Dan M. Marom, *Senior Member IEEE*, Yutaka Miyamoto, *Member IEEE*, David T. Neilson, *Fellow IEEE*, and Ioannis Tomkos, *Fellow IEEE*

ABSTRACT | Forthcoming capacity scaling requirements of optical networks and advances in optical fiber communications beyond the omnipresent single-mode fiber operating over the conventional band introduces new opportunities and challenges for exploiting the expanded spectral and spatial resources available for fiber-optic network designs. The spectral and spatial degrees of freedom introduce utilization tradeoffs that can be leveraged under different applications. After briefly reviewing the supporting network building elements (emerging fiber types, multiplexers, optical switches, and amplifiers), we consider networking scenarios such as intra/inter datacenter, terrestrial, undersea, and wireless 5G/6G hauling networks and identify the best utilization plan and key attributes that can be harnessed by the offered spectral and spatial degrees of freedom for each scenario and how optical switching can be employed therein for traffic management. Networks supporting these scenarios are experiencing tremendous traffic growth pushing their existing implementations to their physical capacity-distance limits. New network builds must offer significant capacity multipliers in an efficient and cost-effective manner, requiring new switching solutions for supporting the unabated traffic growths foreseen in the years to come. We discuss how space-division multiplexed networks can help address this challenge in key communication scenarios.

KEYWORDS | Datacenter networks; multiband communication; optical fiber communication; optical interconnections; space-division multiplexing (SDM).

NOMENCLATURE

AWGR	Arrayed waveguide grating router.
B&W	Black and white.
BBU	Baseband unit.
BU	Branch unit.
CO	Central office.
DLW	Direct laser writing.
DSP	Digital signal processing.
EDFA	Erbium-doped fiber amplifier.
EYDFA	Erbium–ytterbium-doped fiber amplifier.
FP	Fiber pairs.
FSO	Free-space optical.
LC	Liquid crystal.
MCF	Multicore fiber.
MDL	Mode-dependent loss.
MEMS	Micro-electromechanical system.
MIMO	Multiple-input/multiple-output.
MMF	Multimode fiber.
OADM	Optical add–drop multiplexer.
ODN	Optical distribution network.

Manuscript received 23 December 2021; revised 6 May 2022 and 13 September 2022; accepted 15 September 2022. Date of publication 28 October 2022; date of current version 11 November 2022. This work was supported in part by the Research and Development Project commissioned by the National Institute of Information and Communications Technology (NICT) under Grant 18801, in part by the EU-Japan coordinated Research and Development Project on "Scalable And Flexible optical Architecture for Reconfigurable Infrastructure (SAFARI)" commissioned by the Ministry of Internal Affairs and Communications (MIC) of Japan and EC Horizon 2020, and in part by the "INSPACE" Project through the Future Networks Program of the EC Seventh Framework Program. *(Corresponding author: Dan M. Marom.)*

Dan M. Marom is with the Department of Applied Physics, Hebrew University of Jerusalem, Jerusalem 91904, Israel (e-mail: danmarom@mail.huji.ac.il).
Yutaka Miyamoto is with the NTT Network Innovation Laboratories, Nippon Telegraph and Telephone Corporation, Yokosuka 239-0847, Japan.
David T. Neilson is with Nokia Bell Labs, Murray Hill, NJ 07974 USA.
Ioannis Tomkos is with the Department of Electrical and Computer Engineering, University of Patras, Rio Campus, Patras, 26504 Achaia, Greece.

Digital Object Identifier 10.1109/JPROC.2022.3207576

OOK	ON–OFF keying.
OXC	Optical cross-connect.
PAM	Phase–amplitude keying.
PIC	Photonic integrated circuit.
RAN	Radio access network.
RF	Radio frequency.
ROADM	Reconfigurable optical add–drop multiplexer.
RPF	Repeater pump farming.
RRU	Remote radio unit.
SBT	Spatial beam transformer.
SDM	Space-division multiplexing.
SLM	Spatial light modulator.
SMF	Single-mode fiber.
SPOC	Spatial and planar optical circuit.
TTDL	True-time delay line.
UWB	Ultrawideband.
WDM	Wavelength-division multiplexing.
WSS	Wavelength-selective switch.

I. INTRODUCTION

Every action we take sets off a cascade of information exchanges carried on communication networks, whether it is an Internet search engine query, viewing your social media, or just moving about with your smartphone at hand. The information seamlessly flows across wireless and fiber-optic networks, from end users to datacenters and repositories, whether they are nearby or elsewhere around the globe. The increasing populations now connected, the proliferation of applications consuming larger amounts of information, and background machine-to-machine data exchanges are leading to steadfast exponential growth of carried network traffic [1]. This ever-growing traffic, carried by lightwave networks on optical fibers spanning the globe, leads to formidable technical and economic challenges that engineers must face in continuing to scale networks to ever higher capacities [2].

Innovations introduced over the last 40 years have been able to successfully support the fiber capacity growth rates, achieving a million-fold capacity increase based on the introduction of various key technologies such as faster optoelectronic components for higher communication baud rates, WDM and multichannel optical amplification, and in-phase/quadrature multilevel modulation with polarization multiplexing and coherent detection. Such high-capacity optical transport technologies are indispensable in conventional terrestrial core/metro and submarine networks, but also the 5G/6G wireless/wireline access network and emerging datacenter interconnects.

The identification of a physical capacity limit to transmission over SMF in 2010 beset by optical fiber nonlinearities [3], [4] has led to a new research venue capitalizing on SDM [5], [6], [7]. SDM systems introduce new types of fibers and ancillary networking components, supporting additional spatial conduits for information transmission, offering opportunities for capacity enhancements, modified resource allocations, and component-sharing strategies for greater network operation and cost efficiencies. Optical switches required to dynamically route communication channels via lightwave networks operating with WDM and SDM must also evolve to support routing information channels in both the spectral and spatial domains in an efficient manner, matched per application scenario [8].

In this article, we briefly review the fundamental elements required in support of future fiber-optic networks employing WDM and SDM (Section II), followed by an examination of four key networking scenarios of terrestrial systems (Section III), undersea networks (Section IV), fiber hauling networks supporting 5G/6G wireless access (Section V), and intra-/inter-datacenter optical interconnects and networks (Section VI). For these scenarios, we identify the best resource utilization plan and key attributes that can be exploited by the offered spectral and spatial degrees of freedom and the ancillary switching hardware attributes required for supporting their networking implementation.

II. ELEMENTS of SDM-WDM OPTICAL NETWORKS

Constructing cost-effective optical networks requires a careful balance of a multitude of parameters. We focus here solely on the physical layer, the optical hardware responsible for transporting the information-bearing photons, yet some constraints introduced here may have wide-ranging implications for higher networking layers managing functions such as routing and channel assignments. While we focus on spectral and spatial network switching aspects in this article, we first briefly describe the SDM optical fiber solutions and the means to interface to them (multiplex and demultiplex). The main types of optical switches used in lightwave systems and their modifications are described in greater detail in Section II-C. We then complement the optical networking elements introduction by accounting optical amplifiers and transceivers' recent developments.

A. Optical Fibers

The geometry and refractive index distribution of optical fibers dictate their waveguiding properties. SDM makes use of optical fiber links having multiple guided modes: within a single-core supporting multiple spatial modes (MMF), within multiple cores (MCF) arranged within the cladding with each supporting a single spatial mode, or multiple cores each supporting multiple modes [9], see Fig. 1(a). MCFs can be further tailored with identically sized cores (homogeneous case) or differently sized cores (heterogenous case), in effort to control or abate the mutual coupling between closely packed cores. Even grouped SMFs can be considered as SDM network links, with the efficiencies derived from shared components rather than a common fiber platform. When considering the implications of the fiber properties toward the optical network function, the primary attribute of attention is

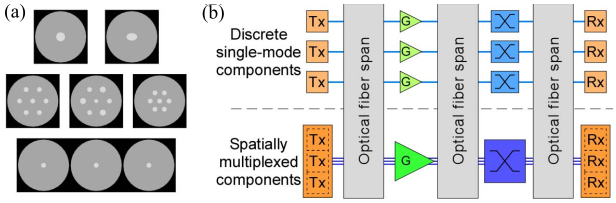

Fig. 1. *(a) Optical fibers supporting SDM transmission: MMFs, with circular and elliptical cores (top row); MCFs, with homogeneous, heterogeneous, and coupled cores (center row); and array form of SMFs (bottom). (b) Spatially parallel optical communication system having transmitters, amplifiers, switches, and receivers. Said components can be discretized per spatial channel (top) or made SDM compatible (bottom) and interconnected by an SDM optical fiber link of choice.*

whether the guided modes intermix or not. Should mode mixing occur at the physical layer (whether by the optical fiber or ancillary components), then the entire mixed mode set must be routed through the network as a single entity, between SDM transmitter and receiver, as postdetection DSP would need to be applied across the mixed spatial set to unravel the transmitted information channels. This constrains the network routing flexibility but may allow for optical switch sharing as the same routing destination is applied across the mixed modes. Degenerate spatial modes in MMF exhibit strong mixing in fiber propagation, whereas bundles of SMF cannot mix within the fiber medium. Other SDM fiber designs can control the level of mixing, enhancing, or attempting to suppress it. In homogeneous MCF, setting the identical cores in close proximity results in strong coupling [10] (strong coupling advantageously reduces mode- and polarization-dependent losses and limits differential delay spread [11]), whereas adopting a heterogeneous design and increasing the core pitch reduce the coupling [12]. In MMFs, mode mixing can be suppressed by breaking mode group degeneracy [13], [14]. While the fabrication of MCF is more intricate than single-core fibers (SMF and MMF), advanced manufacturing processes have led to fiber losses on par with SMF, for both coupled [10] and uncoupled [15] types. Noteworthy transmission capacity records for SDM fibers include 19 cores with each supporting six modes within a 267-μm-diameter fiber demonstrating 10.16 Pb/s [16], four single-mode core fiber within a 125-μm standard outer diameter fiber transmitting 1-Pb/s traffic [17], and single-core, 15 spatial mode fiber having a standard 125-μm cladding diameter with a 1-Pb/s capacity [18].

B. Space-Division (De)multiplexers/Fan-In (Out) Devices

The optical modes/cores within SDM fibers need to interface to discrete spatial channel sets of the same dimension outside the fibers. This occurs at the transmitter and receiver sites, which are single-mode-based (and may share common DSP [19]), but may also be required at intermediate network locations where some components such as optical amplifiers and switches that are not adapted to the SDM fiber may be deployed. Possible deployment arrangements utilizing discrete components as well as SDM-converted components with network links utilizing SDM fibers or the parallel SMF alternative are shown in Fig. 2, with placement of spatial multiplexers/demultiplexers where needed for format adaptation. The implementation choice for SDM-adapted fibers and components over parallelism of SMFs and devices is ultimately dictated by system constraints, such as cost, size, power consumption, and supplier availability.

Interfacing MCF, especially with single-mode cores, is relatively simple and can be accomplished by an imaging operation using lenses [20]. Alternatively, SMF groups can be drawn down to a reduced pitch, matching the core positions of the MCF and then directly spliced [21], [22]. A more compact realization of pitch reduction can be achieved by 3-D waveguides inscribed within an optical glass block using the DLW technique [23]. Such fan-in/fan-out devices between multiple SMFs and an MCF achieve very low loss but are serially manufactured making their mass production challenging. This is one of the motivations for adapting networking components to interface directly to the SDM fiber,reducing the need for spatial multiplexers. As an example,multichannel transmitters and/or receivers may be integrated onto a single PIC,which can then directly interface to MCF via an array of grating couplers radiating normal to the planar circuit [24]. Although grating couplers have higher losses and introduce wavelength and polarization dependencies,this demonstrates the potential for additional functional integration in PIC platforms.

In support of MMF interfacing to parallel SMF, an optical functionality of mode demultiplexing is required. Since the spatial modes often intermix throughout transmission in MMF, the mode demux does not necessarily have to map each mode to a particular SMF of the array as DSP would be employed to unravel the mixed spatial communication

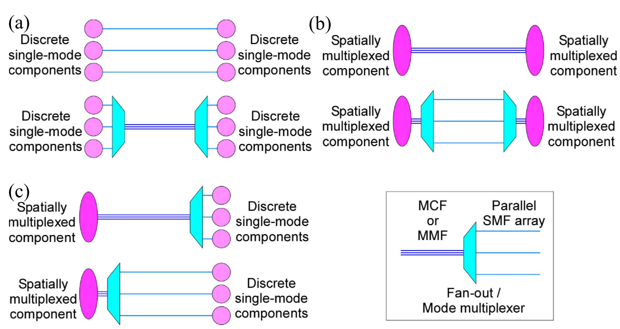

Fig. 2. *Connectivity options between SDM/discrete components and fibers. (a) Discrete components, attached by parallel SMF or SDM fiber with spatial multiplexers, (b) SDM components, directly attached to SDM fiber or parallel SMF with spatial multiplexers, and (c) discrete components connected to SDM ones, with SDM or parallel SMF, determined by the position of the multiplexer.*

channels. The most important attribute for the mode multiplexer is minimizing its MDL, as MDL directly leads to reduced information capacity [25]. Nevertheless, both mode mixing and mode preserving spatial demultiplexers have been developed. The technique of inscribing 3-D waveguides in glass using DLW can be used to construct photonic lanterns, which consists of an adiabatic spatial transition from a multimode optical waveguide to a discrete set of single-mode waveguides with matching mode and waveguide counts [26]. Photonic lanterns can also be realized by drawing multiple fibers encased in a lower refractive index capillary to an MMF that can be directly fiber spliced [26]. Alternatively, multiple encoded phase plates can transform at low loss between single-mode input sources/optical beams and a mode multiplexed output [27]. Due to the 2-D modal field distribution of MMF, realizing PIC-based multiplexers is more challenging, but examples have emerged [28].

C. Optical Switches

Optical networks are composed of fiber links connecting geographically distributed sites where switching nodes are disposed. In today's WDM-based networks, carried over SMF, the switching functionality is called ROADM node. ROADM nodes employ multiple $1 \times N$-port WSSs in a route-and-select topology [29], where N is the output port count (a distributing WSS on each ingress fiber and a combining WSS on egress fibers combine for a Spanke-topology architecture [30] per wavelength). Internally, WSS spatially disperses the input fiber spectrum for accessing the optical bandwidth of each WDM channel and beam-steer each wavelength channel to the desired output port (out of N) using a pixelated SLM. Using an SLM enables the WDM channel spacings and bandwidths to be software-defined (and in-field modified, i.e., flexible-grid property [31]), making them future-proof as higher baud rate transmission rates and new WDM channel plans emerge, but the SLM switching technology is relatively slow (millisecond rate). WSS variants based on WDM channel demultiplexers followed by discrete space switches do not support flexible grid operation but allow the introduction of faster switching technologies, e.g., microsecond and nanosecond switching times [32], [33]. This demonstrates how different features of an implemented switch can be leveraged for diverging networking requirements.

The trend of terrestrial network node throughput growth places extra strain on the ROADM switching capability (see Fig. 3), as more fibers (and possibly associated spatial modes) and higher capacities are routed at network nodes. By the end of this decade, network nodes will be required to route ~10 Pb/s carried over a large number of fibers and expanded operating wavelength ranges. In support of multiband optical communications, free-space WSSs are being redesigned to span the wider band communications while maintaining low losses and fine spectral resolution across the operating band [34].

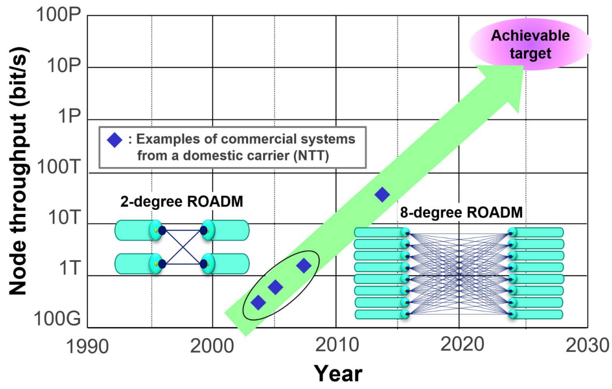

Fig. 3. *Optical node throughput growth trend. The node throughput is the product of number of fiber ports, number of spatial lanes, number of wavelengths, and bit rate per wavelength.*

Integrated WSSs operating with multiband demultiplexers have recently been demonstrated, using overlapping diffraction orders of the demultiplexers [35]. In support of SDM transmission, as more parallel spatial channels exist per link, the number of WSS output ports must increase as well to address all switching directions and spatial lanes. However, the complexity of WSS scales with the number of addressable spectral points (=supported bandwidth/optical resolution) and the number of output fiber ports. Any increase in one metric or the other necessarily leads to larger, more complicated WSS switches. This makes it challenging to support wider band communications at the same optical resolution (increases addressable spectral points) and SDM (which requires an increase in the fiber ports).

When considering the channel switching/routing about an SDM/WDM optical network, we must first consider whether the optical communication channel may introduce mode mixing, whether in SDM devices or fiber. If no-mode mixing occurs, then each guided mode can be independently routed toward its destination, which can be achieved by placement of a WSS per spatial lane [Fig. 4(a)]. This implementation can be economized by array integration of multiple WSS in a single module [36], [37]. In case spatial channels intermix, then all the mixed spatial channels must be switched jointly as the information is potentially spread across the mixed channel set. Joint switching can be performed by prescribing the same switching assignment to each WSS disposed on the mixed SDM group. However, the individual switched paths (carried on separate fibers) should be of equal length to eliminate delay spread, which would exacerbate the DSP load. Furthermore, even though there are individual WSSs capable of independent switching, in mixed channel transmission, we are constrained to switch jointly and hence do not exploit the independence property. These shortcomings can be eliminated by adapting a single WSS to jointly switch spatial channel sets [Fig. 4(b)]. WSSs adapted for joint switching and being interfaced to MCF [38] and MMF

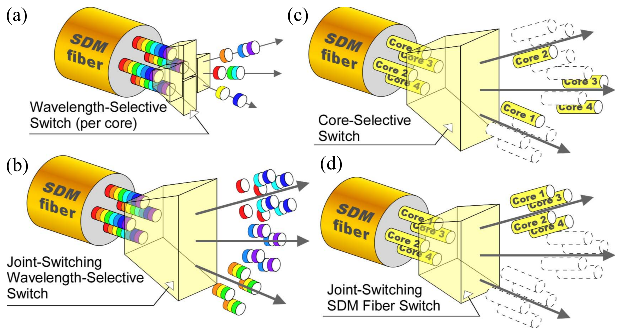

Fig. 4. ***Channel switching options for an ingress SDM/WDM optical fiber of an optical network node. (a) Independent wavelength routing per spatial core. (b) Joint wavelength routing across all cores. (c) Core switching, of entire optical spectrum. (d) Complete fiber contents switching.***

[39], [40] have been demonstrated. Returning to the no-mode mixing scenario, then switching at the granularity of single cores can be devised, leading to a core-selective $1 \times N$ switch [41], enabling a route-and-select topology at the spatial lane level [Fig. 4(c)], as performed today in today's SMF networks at the wavelength channel level. The tradeoffs between independent switching of each wavelength and core communication channel at the expense of hardware complexity versus switching at the wavelength channel level across all spatial channels (known as wavelength superchannel) or at the spatial channel level across all wavelengths (spatial superchannel) have been addressed in [42] and [43] and remains an active area of debate for future network builds.

A different class of fiber switches establishing $N \times N$ connections, or OXC function, can be used to route entire fiber contents (without accessing the WDM layer). OXC-based nodes can replace WSS route-and-select nodes when network traffic is allocated in full fiber assignments. Since today's Internet router blades have <1-Tb/s line rates, it is still more efficient to wavelength multiplex many channels onto a network fiber. Yet, with router interfaces increasing at a 40% yearly rate [44], by 2030, we should see a few tens of terabit-per-second router interfaces that may be efficiently allocated to full conventional-band (C-band) SMF. Under this scale, optical networks will potentially route full fibers with OXC disposed at nodes. High port count, free-space-based OXC with beam-steering MEMS micromirrors were developed during the telecom bubble era [45], [46], offer millisecond switching rates, and more recently were demonstrated in an integrated form and wafer scale with microsecond switching rates [47]. OXC based on SMF ports can be used for routing in SDM-based networks, in scenarios where entire spatial channels are routed (spatial superchannels that have not experienced mode mixing), by spatially demultiplexing the SDM traffic prior to switching. Free-space OXC can be readily adapted to support full SDM fiber content switching under joint-switching scenarios, thus saving OXC fiber ports and applicable for mode-mixing scenarios [Fig. 4(d)]. Joint-switching OXC was demonstrated for low-core MCF [48] and its scaling potential to high core and port counts has been studied [49]. Conceivably, free-space OXC can be designed to switch between MMF I/O ports.

D. Optical Amplifiers

Optical fibers exhibit propagation losses that can be compensated by optical amplification to achieve extended transmission distances. Lightwave systems employ EDFAs, which offer an operating bandwidth of few terahertz, from which the C-band with around 5 THz is defined. EDFAs' key attribute is that it amplifies all the wavelength channels within its operating band, potentially many tens to one hundred channels, allowing one lumped device to extend the reach of optical fiber communications from tens of kilometers to potentially thousands of kilometers. EDFAs can also be operated in a longer band (L-band), which provides another approximately 5 THz of bandwidth. Fiber capacity can be further increased by expanding the available gain bandwidth via the introduction of other amplifying means, such as new rare-earth dopants, Raman amplifiers, or semiconductor optical amplifiers [50]. Each optical amplification solution covers only a finite bandwidth, necessitating the separation and recombination of the multiple bands at each amplification site and the deployment of disparate amplifying technologies. While such a solution may not be as elegantly implemented as EDFA, this multiband solution does extend the capacity of already deployed SMF by a small, single-digit factor and provides a near-term, cost-effective solution for network operators [51]. SDM transmission increases capacity by the introduction of guided modes, offering a larger capacity multiplier potential (in contrast to multiband transmission), but can capitalize on the C-band where erbium-based optical amplifiers are the most mature technology. Amplification of SDM transmission can be accomplished by array forms of EDFA, one per guided mode and possibly sharing common pumping lasers [52], or by erbium-doped MCF or MMF optical amplifier variants [53], [54]. Single-mode array-form EDFAs allow the individual gain per fiber to be actively controlled but require the fan-in/fan-out of the MCF cores (or demux/mux of the MMF modes) of the SDM solution at each amplification site (but is readily compatible with SMF arrays). MCF and MMF EDFAs require special geometric designs to achieve low mode or core-dependent gain.

E. Optical Transceivers

Optical transceivers are the line termination units, where the optical signal is generated or terminated and electronically interfaced to routers and data switches. As the capacity of line interfaces increases beyond the single wavelength optoelectronic conversion capability, multiple carriers are integrated in higher capacity optical transceivers. These carriers can be separate wavelengths to be

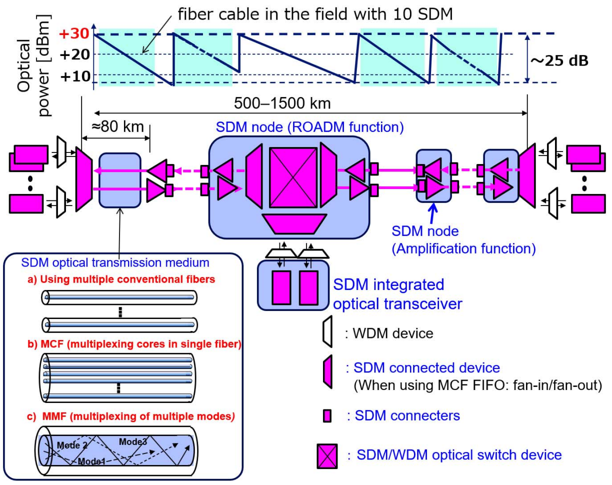

Fig. 5. ***Future terrestrial SDM optical transport network, showing the optical fibers, optical amplifiers, optical switches, and line terminating units, all adapted for SDM.***

multiplexed onto SMF or interfaced to a parallel fiber connection (or SDM fiber) utilizing a single wavelength source. Wavelength multiplexed transceivers can be based on multiple laser sources [55] or a single-frequency comb source [56]. Likewise, SDM interfaced optical transceivers can be based on multiple laser sources [57] or a single intense source shared for all [58]. If the SDM transmission fiber will experience mode mixing,having a common laser source is advantageous for the postdetection DSP required to unravel the original information,as their phase relationship is common.

III. TERRESTRIAL NETWORKS

By 2030, the required transmission capacity and optical node throughput for terrestrial networks are expected to exceed 1 and 10 Pbit/s, respectively, as shown in Fig. 3. SDM is one of the most promising technologies to scale not only the total system capacity and reach but also the network node throughput in the future.

A. Advantages of SDM in Terrestrial System

An overview of a terrestrial optical communication system employing SDM is shown in Fig. 5. Terrestrial systems, in general, exhibit large variability across its network link lengths and node connectivity degree to neighboring nodes (both being generally defined by geography), and link loads and add/drop capacity (defined by traffic requirements). This prevents terrestrial networks from adopting a highly optimized design, as the system implementation needs to effectively accommodate the different requirements at each node using the same design and equipment. This is in contrast to datacenter application and in submarine systems, whose architecture and traffic patterns obey very uniform design attributes. In terrestrial systems, the use of multiple conventional fibers in array form is the likely near-future option for the fiber transmission media. MMF and MCFs are attractive to offset the physical limits of SMF systems and enhance the spatial density of optical fiber cabling, yet these features are more compelling in datacenters and submarine systems. SDM also offers the opportunity to reduce the size and power consumption in the network equipment such as optical transceivers, inline amplifiers, and optical routing nodes.

In consideration of the total power level diagram of Pbit/s-class link capacities, output powers in excess of 1 W or +30 dBm have to be carefully managed in telecom operation and telecom environment maintenance actions while keeping the laser safety for both telecom facilities and network operators. High-output power management inside the network equipment can be more manageable than in the telecom field environment, where the output powers of the equipment are limited to satisfy laser safety criteria.

B. SDM Transmission Capacity Aspect

Transmission capacity can be scaled to 1 Pbit/s level by directly utilizing uncoupled MCF [59], with each core of the uncoupled MCF having almost the same optical properties as SMF, and hence, today's digital coherent transceivers can be immediately utilized. The number of parallel cores can reach 32 within a cladding diameter of 250 μm, where the mechanical reliability of MCF can still be guaranteed [60]. Alternatively, utilizing 32 SMF (of 125 μm diameter), tightly packed, would require a minimal diameter of 850 μm (without considering the jacket coating protecting individual fibers, which would increase the diameter twofold, at least). Careful consideration of the core-to-core crosstalk is managed by incorporating a heterogeneous MCF arrangement (based on two core types), reducing the intercore crosstalk. As a result, the required bandwidth for 1-Pbit/s capacity can be supported by $\sim$4.5 THz of the conventional communication band, employing dual-polarization 16-QAM constellation size. With the optical bandwidth spanning the C-band, simple 1-Pbit/s SDM inline amplified transmission can be conducted over a 200-km distance; if the modulation format is set to 8D-16QAM format, the transmission distance can be extended over 1200 km with a capacity of 0.75 Pbit/s. Virtual three-node SDM network experiments were also demonstrated using conventional WSS developed for SMF networks [61].

A key element of the terrestrial SDM network is an SDM-adapted optical amplifier. Cladding-pumped MC-EYDFA (erbium and ytterbium ion doped) inline amplifiers are one of the promising technologies and several challenges have been addressed to reduce the size and power consumption of the optical inline amplifier. Fig. 6 shows one example to the reduction of MC-EYDFA power consumption by increasing core number to more than 30 [53]. The vertical axis shows relative power consumption of MC-EYDFA. The solid line of slope 1

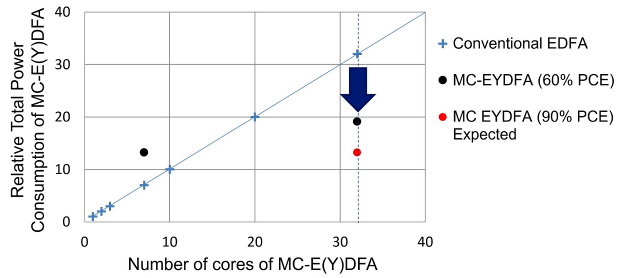

Fig. 6. ***Reduction of power consumption of MC-EYDFA by increasing core counts. PCE: pump-power coupling efficiency.***

shows the linear power consumption scaling of multiple conventional EYFDAs. In the case of seven-core EYDFA, the power consumption of cladding-pumped MC-EYDFA is higher than that of multiple EDFAs. On the other hand, 32-core EYDFA can reduce power consumption compared with the multiple EDFAs. This efficiency improvement for cladding pumping originates from increasing the effective area of active cores. Another work showed improvement of cladding pump efficiency for 19-core EDFA in C- or L-band [62]. Here, very uniform gain and noise figure spectra across either full C-band and full L-band were demonstrated based on a typical Er-doped fiber amplifier. By increasing the core number from 7 up to 19, cladding pump efficiency can be improved by 0.9 dB in the C-band and 2.7 dB in the L-band. A technoeconomic analysis of a common MC-EYDFA having 12 cores versus a bank of single channel amplifiers turned on sequentially as capacity dictated demonstrated that while an initial investment and upfront costs may be higher, the common amplifier brings the long-term profitability of 33% and 55% power savings [63].

The advantages and simplicity behind cladding pumping of MCF optical amplifiers are countered by the possibility of a gain imbalance. One technique for obtaining uniform gain and low-core-dependent gain in cladding-pumped MCF is with strongly coupled cores [64]. However, introducing strong coupling optical amplifiers necessarily converts the spatially parallel communication system to a coupled one, which impacts the ability to independently route and detect spatial channels. Another option is to introduce core-by-core dynamic gain control. In [65], the introduction of cladding and core hybrid pumping scheme was proposed. Two types of hybrid pumping schemes, namely, one-stage hybrid pumping and two-stage hybrid pumping, were tested. There was no significant difference between the hybrid-pumped MC-EDFAs and the reference conventional EDFAs in dynamic gain change rate, where the cladding-pumped power is not adjusted and kept constant. Another interesting feature of the cladding and core hybrid pumping is the reduction of power consumption; de Gabory et al. [66] demonstrated 30% power saving of the hybrid pumped MC-EDFA by introducing proper control of the hybrid ratio of cladding pumping versus core pumping, depending on the monitored temperature of MC-EDFA, considering the ambient temperature change in real telecom facilities.

Multivender interoperability transmission test using four-core SMF and connectors having standard 125-μm cladding diameter was demonstrated in the combination of cladding-pumped seven-core EDFA inline repeaters [67]. Four-core fiber splicing and four-core fiber terminated with standard SC/MU-type connectors were also demonstrated by three different fiber manufacturers under common specification. The average loss coefficient of 0.21 dB/km was achieved, almost the same as that of conventional SMF. Seven-core cladding-pumped EDFA inline repeaters were tested to show 16% power-saving performance. The 118.5-Tbit/s transmission capacity experiment was achieved with MC-EDFA within the C-band over distance of 300 km.

C. SDM Optical Switching Node Aspect

Future OXC switches may be required to accommodate several types of switching granularity demands, requiring a multigranular (layered) OXC structure to be employed [68], [69], consisting of wavelength switch, wavelength-band switch [70], and spatial switch. In the future, when huge optical path capacities with over 10 Tb/s will dominate, a spatial switch-based SDM OXC architecture will become very efficient [71], [72], [73]. For a smooth migration from today's WSS-based networks to future SDM networks, scalable architectures are important aspects to be addressed [74], [75].

A scalable OXC node based on $N \times N$ WSS modular subsystem was proposed, as shown in Fig. 7 [76]. In conventional ROADM nodes employing the route-and-select architecture, $2M$ sets of high-port-count $1 \times M$ WSS are required for cross-connecting M-SDM channels, for realizing large-scale switching nodes. In addition, high-fiber-count (M^2) optical mesh interconnections must be accommodated. Alternatively, the architecture based on subsystem configuration requires medium-size $N \times N$ WSS subsystems, and the subsystem modules are connected according to the traffic demand. To realize such compact SDM switching nodes based on the architecture, N-lane

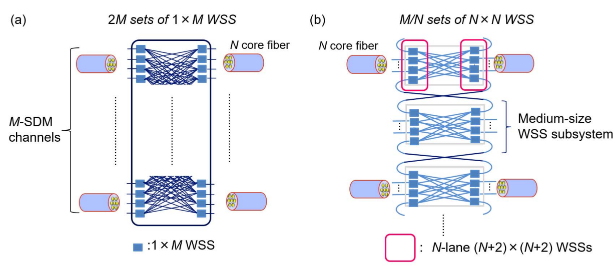

Fig. 7. ***Large-scale wavelength switching for SDM network nodes. (a) Conventional route-and-select based on high-port-count WSS. (b) Switching architecture based on N × N WSS modular subsystem.***

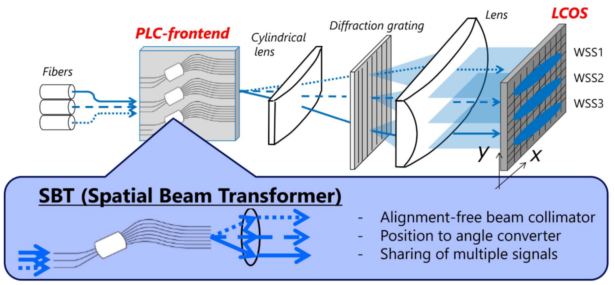

Fig. 8. *Integration of multiple WSS units based on hybrid optical platform of waveguide and free-space optics utilizing SPOC platform.*

$1 \times N$ WSS integration technologies using a novel technology called SPOC have been proposed and tested [77].

The SPOC platform is highly suitable for integrating multiple WSSs in one module, as shown in Fig. 8. It has a configuration combining a waveguide and free-space optics and is composed of PLC front ends, a cylindrical lens, diffraction grating, a lens, and a switching engine. An SBT is used as a beam launcher. The SBT has the same circuit structure as an AWGR, except that the path-length difference of the arrayed waveguides is set to zero. It, therefore, does not disperse light spectrally but forms an extended output beam profile and the output propagation direction is determined by the input waveguide position due to the spatial Fourier transform property of the slab lens. The SBT circuit has two important functions: a position-to-angle converter and the sharing of multiple signals. Due to these advantages, a WSS array function was integrated into one compact module [78].

Several optical configurations for system integration are possible. The first system implementation is based on a "2-f optical system." A 2-f optical system utilizes a single lens. The light reflected by the switching engine is coupled to a different SBT depending on its reflection angle. In this system, an SBT is shared by all WSSs in the module. Thus, the same port numbers of different WSSs are adjacent to each other. The second-type system is called a "4-f optical system." In 2-f optics, an SBT is solely used to construct a certain WSS.

A 4-f optical system utilizes two lenses, so the optical signal output from an SBT is reflected by the switching engine and returned to the same SBT. This means that the SBT is occupied by only one WSS in the array. Therefore, the ports belonging to the same WSS are adjacent to each other.

The concept for the integrated $N \times N$ subsystem modules is proposed and demonstrated with simplified optical wiring with no degradation of loss and cost, as shown in Fig. 9 [79]. The conventional configuration, based on route-and-select, utilizes $1 \times N$ and $N \times 1$ WSS with full mesh interconnecting fibers, requiring complicated optical wiring which makes fabrication and maintenance difficult. To solve this problem, 2-f SPOC-WSSs at the input feed into 4-f SPOC-WSSs at the output, obtaining an asymmetric port arrangement. As a result, full mesh optical wiring in $N \times N$ WSS can be eliminated, and simple straight optical wiring can be realized. This architecture recently demonstrated $N \times N$ WSS subsystem switch module scaled up to 10×10 port counts, based on a single 4K-SLM device [80].

IV. UNDERSEA SYSTEMS

In an ever-connected world, information communicated between continents is experiencing explosive growth, leading to many new undersea cable installations of longer range and higher capacity, connecting more endpoints than ever before. A survey on submarine cable technologies can be found in [81]. A survey on SDM's potential role in transoceanic cable systems can be found in [82]. Several experiments are mentioned, e.g., an SMF transmission of 65 Tb/s over a 6600-km distance and another of 70.4 Tb/s over a 7600-km distance. The conclusion is that the only way toward higher capacities is to expand either to a wider range of bandwidth, thus a UWB transmission system, or to a wider space dimension by incorporating more spatial lanes (SDM). The debate as to which type of system (UWB or SDM) will prevail, for either terrestrial or submarine networks, is ongoing [83]. It is expected that within the next 3–4 years, submarine cables containing 40 fibers or more and within the next 5–7 years containing MCFs will need to support trans-Atlantic distances with capacities of 1 Pb/s, while the capacity needs to scale-up to about 5 Pb/s at by 2030 with cables containing about 200 fibers or cores. The benefits of advanced undersea networks extend also to shorter scenarios, e.g., Mediterranean Sea network scale [84], [85]. In specialized, low-latency applications, hollow-core fibers may be introduced.

Besides the quest for higher capacity systems that is the common goal for both terrestrial and submarine networks, the power limitations in operating submerged networks are a critical issue that must be dealt with in scaling system capacity in submarine networks. A significant part of power is consumed at the submarine network repeaters (currently utilizing full C-band or C + L-band EDFA technology, but in the future is expected that C + L-band systems will be increasingly utilized) that today are capable of

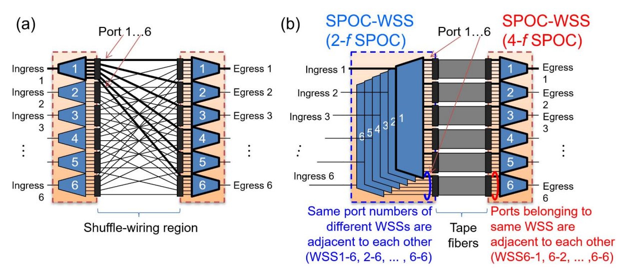

Fig. 9. *Optical wiring comparison for N × N WSS subsystems. (a) Implemented with arrays of 1 × N and N × 1 WSS. (b) Using asymmetric 2-f/4-f integrated SPOC systems as modular modules.*

supporting (alongside with the other mature transmission technologies) distances up to 15 000 km with amplifier spacings ranging between 60 and 110 km. However, the maximum voltage available from the shores (up to 15 kV) and cable resistivity (note that the cable contains a layer of conductor used to supply current to the repeaters) limit the amount of available power to the repeaters [86]. Increasing the number of fibers in a submarine cable can be used to increase the capacity of the cable at constant power because of logarithmic dependence of the Shannon capacity formula and the limitations of nonlinearity [87]. For example, replacing a single fiber operating close to the nonlinear limited capacity with two fibers operating at half the launch power will give a capacity increase of around 70%–80% at constant system power.

Finally, the nature of undersea installments has traditionally been as straight trunks interconnecting continents, with all networking functions implemented upon landfall. This is beginning to change with the introduction of undersea branches serving several geographical sites with the same fiber. Such branches can be implemented with predetermined and fixed wavelength allocation (add/drop), which can be set by passive optics means. Placement of a reconfigurable wavelength management unit affords greater flexibility and adaptability to fluctuating demands, and however, a major concern for undersea systems is their reliability due to the impact of equipment failure in down time and repair cost.

The era of undersea SDM systems deployments for the implementation of high-capacity submarine networks has already started [88]. The first generation SDM-based submarine systems have started being deployed since 2020, before any terrestrial SDM network of any kind, and are based on bundles of parallel SMF. The fabrication technology of SMFs for undersea cabling advances and currently 200-μm coated SMF fibers are commercially available, while it is expected that soon 140-μm coated SMF fibers will be commercialized [83]. Such reduction of the coating diameter is expected to double the cabling density, so a spatial density capacity boost is expected, compared to current cable designs, in the sense that more fibers can be packed in the available space within each cable [Fig. 10(a)].

Greater spatial density can be obtained from specialized SDM fibers, namely, cables incorporating MCFs or MMFs. However, at present, these SDM fibers introduce higher losses, which subsequently will require improved amplification that can result in higher power requirements for the repeaters. Consequently, cables with even higher power handling (conductivity improvement via larger cross section) will need to be deployed, which introduces other problems. In addition, one needs to consider that MCF-/MMF-based SDM systems will employ repeaters with higher noise figure while introducing also other performance degrading phenomena, e.g., mode-dependent gain (MDG)/MDL. Such considerations add to the concerns that MCF-/MMF-based SDM systems might require

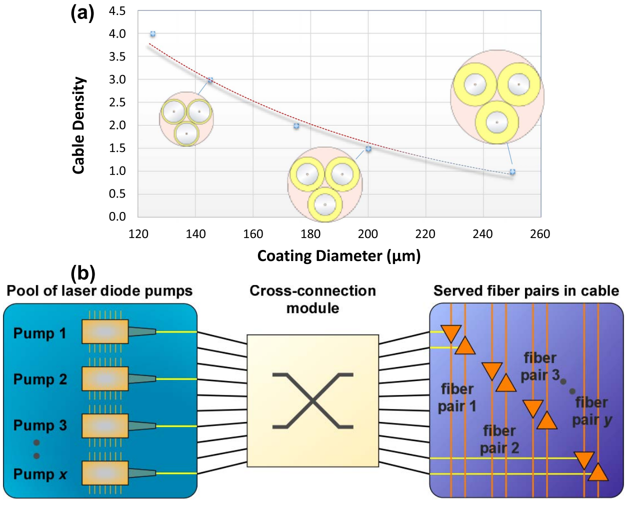

Fig. 10. *(a) Improvement to cable density as thinner fiber protective coating technology is introduced. (b) RPF example utilizing a pool of x laser diode pumps to serve fiber amplifiers on y FPs, interconnected by a passive coupler network or active OXC.*

additional technology improvements, longer standardization times, higher qualification time, more training, and so on in addition to power-hungry transponders requiring higher power/cost DSP. Thus, considering these issues, the cost/power consumption benefits of moving to SDM systems based on MCFs/MMFs for submarine applications are open questions [89], [90]. Nevertheless, it is worth noting a system advantage for strongly coupled MCF, which have lower nonlinear penalties (i.e., nonlinear phase distortion accumulation due to the strong mixing phenomena) compared to single-core/fiber transmission, allowing higher SNR and/or transmission ranges and have recently been used for transoceanic transmission distances with real-time MIMO-DSP [91].

The spatial integration/sharing of resources that the current generation of SDM undersea systems incorporate is implemented at the submarine optical amplifiers via the so-called RPF technique. RPF consists of a group (named "farm") of pumps that are cross-connected to each other with either a fiber coupling network that distributes laser pump power to all EDFAs serving the FPs or an active fiber switch. Fig. 10 shows a diagram of an RPF system, which is expected to be in use in all future subsea cable systems announced so far.

Each RPF farm supports a certain group of FPs and utilizes a group of optical pumps that are shared among groups of FPs. RPFs are capable to continue pumping FPs even in the cases that one or more pumps fail, offering a promising solution for network survivability, by assuring redundancy that can maximize network efficiency. It is worth mentioning that more complex subsystem designs including not only sharing of pump lasers but also full EDFAs have already been announced. This technique highlights the acceptance of placing an OXC switching element as reliable for undersea installments and can effectively

Table 1 Available Pumping Schemes

Pumping Scheme	Acronym	Use of Core Pumping	Use of Clad Pumping	Comments
Individual Core Pumping	ICP	Yes	No	*Conventional system*
Shared Core Pumping	SCP	Yes	No	*With 3 dB coupler*
Variable Shared Core	VSCP	Yes	No	*With tunable coupler*
Common Cladding Pumping	CCP	No	Yes	*Need of core attenuation*
Hybrid with Individual Core Pumping	HICP	Yes	Yes	
Hybrid with Shared Core Pumping	HSCP	Yes	Yes	*With 3 dB coupler*
Hybrid with Variable Shared Core	HVSCP	Yes	Yes	*With tunable coupler*

protect against failure of the optical pumps making up the RPF. Protection schemes against pump failures are also possible with passive combiners, namely, merging the main and backup pump lasers with a passive -3-dB coupler network to simultaneously serve several fiber amplifiers. An active undersea switch provides protection against higher pump laser failure counts and improves the system's power efficiency.

RPF technique consists of sharing "x" repeater pumps ($x > 2$) with "y" FPs ($y > 1$) (while in a conventional network, two pumps, main and reserve, are dedicated to one single FP). Several RPF configurations have been explored [92]:

1) four pumps/two FPs and four pumps/four FPs;
2) eight pumps/four FPs and eight pumps/eight FPs;
3) 16 pumps/eight FPs and 16 pumps/16 FPs.

Table 1 shows the characteristics of various announced pumping schemes (depending on the type of pumping they employ; being either core or cladding, or hybrid pumping) for amplified SDM cable systems [93].

The whole process of the design and implementation of a submarine optical cable system is analytically presented in [94]. All stages needed for the construction of an underwater network infrastructure are addressed: route and cables selection, topology design, submarine water-resistant housing for repeaters, branching unit's specifications, proper repeater's spacing definition, power feed equipment (PFE) selection, powering architecture design, ship operations organizing, proper control, monitor and terminal equipment's specifications, and final selection. The last stages are to consider the initial and final targets and select from all available options in order to meet the design specifications. Cable design consists of selection of FPs.

Submarine networks are now expanding from point-to-point connectivity to employing OADMs to enable BUs with bandwidth management, where it is required [95]. Usually, a submarine OADM node contains both a BU and a wavelength management unit (Fig. 11). FPs may bypass the node (through the BU) if are routed directly to other destinations or may enter the node to be switched through the WMU BU to their destination (i.e., south–east destination in Fig. 11). If an OADM node is in a network area, which does not have direct connections to remote destinations, it may have the WMU unit disabled or even not installed at all, compromising the control. Although flexibility may lead to higher cable utilizations in the case of a reconfigurable OADM, strict security protocols must run to prevent unwanted or faulty node configurations and possible unauthorized access.

Land-based ROADMs use WSSs to switch traffic. However, WSSs have a few challenges for operating in the undersea environment. WSSs utilize the LC-based SLM technology for flexibly accessing individual wavelength channels. However, LC-SLM operates over a single polarization state, requiring the use of polarization diversity (doubling the number of beams) inside the WSS, which increases complexity and package size. Moreover, LC remains fluid or "liquidy" at room temperatures and above, whereas at lower temperatures, such as those in the undersea environment, it becomes viscous. To continue operating LC-based devices in cold ambient conditions, a local heater drawing several watts is required. Thus, the size and power draw of LC-SLM employed in WSS make them poorly suited for undersea operations. A recent announcement of WSSs qualified for undersea installations [96] enables reconfigurability to undersea networks with flexible channel plans, i.e., the capability to allocate the fiber spectrum at 3.125-GHz granularity. This is likely possible via the use of alternative SLM technology, based on MEMS tilting digital micromirrors [97], which supports low port count WSSs that are sufficient for BU uses and does not require polarization diversity or an extraneous heater.

V. NETWORKS SUPPORTING 5G/6G WIRELESS ACCESS

The increasing number of mobile devices worldwide, the demand for high-speed access, and the reduced latency

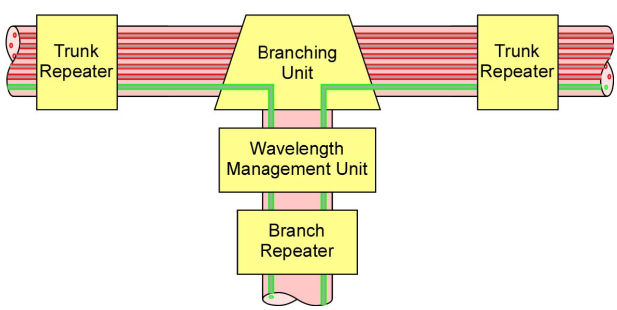

Fig. 11. *Submarine BU and wavelength management unit logical diagram.*

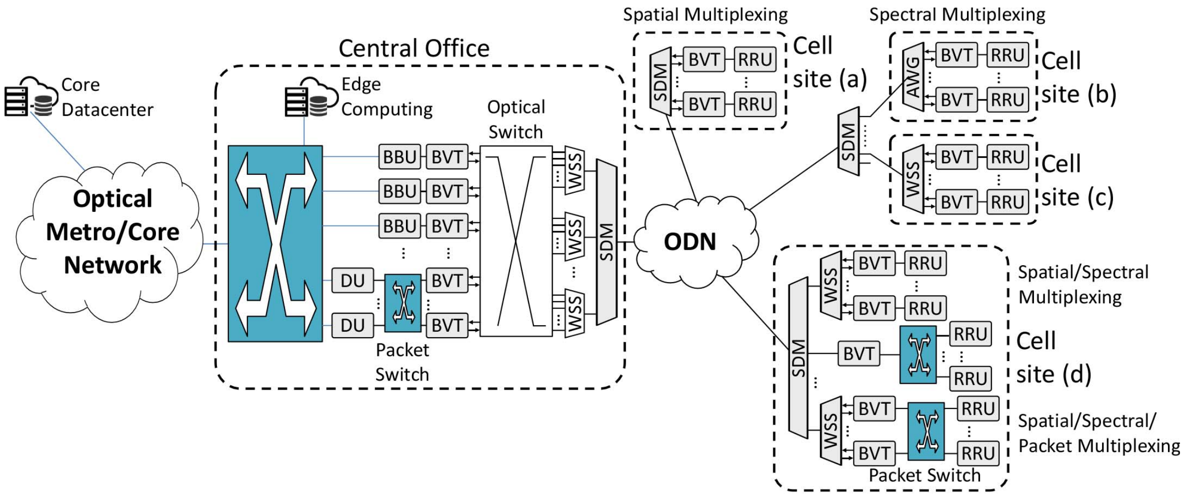

Fig. 12. *SDM/WDM fronthaul network with different multiplexing and demultiplexing options at cell sites: (a) pure spatial multiplexing, (b) spectral multiplexing based on fixed wavelength channels, (c) reconfigurable wavelength channels, and (d) combined spatial and spectral multiplexing with optional packet multiplexing. After [101].*

requirements for running services have been the driving forces for the evolution of wireless technologies. Scaling studies suggest the volume of mobile data (growing at 60%/year [44]) will reach 5 zettabytes per month in 2030 [98]. While the global deployments of 5G are in full earnest, the emergence of Internet-of-Everything (IoE) services is expected to place new constraints of diverging nature necessitating the integration of computing, control, and communication functionalities in a single network design. A review of the key enabling technologies supporting 6G networks can be found in [99], emphasizing millimeter-wave (mm-wave) communications, THz communications, and optical wireless communications, among others. Adoption of these technologies demonstrates a transition to shorter wavelength free-space communications that allow for more advanced antenna designs, enabling the reduction in cell sizes, as well as the use of MIMO signaling or beamforming to increase the signal-to-noise ratio or received powers [100]. This further suggests that the underlying RAN has to transport higher frequency carriers with larger RF bandwidths at denser deployments due to smaller cells, stressing the capabilities of the fronthaul feeder network to deliver up to 1000× more capacity, to support a significantly larger number of users per area, to reach multi-Gbit/s end-user data rates, and to reduce latencies down to 1 ms.

The capabilities of the fronthaul segment of wireless networks can be significantly enhanced by the introduction of SDM, increasing the available degrees of freedom for multiplexing, routing, and slicing data streams, and by the transmission of analog RF information to the antennas in place of digitally sampled information [101]. A generic scheme for the SDM/WDM fronthaul section is shown in Fig. 12. The CO serves as the gateway between the backhaul terrestrial network and the fronthaul comprising part of the RAN. Antenna cell sites (or remote units) are attached via an ODN, here enhanced with SDM. 5G and future 6G network traffic flows to/from the RAN sites via the fronthaul to aggregation routers that are connected to the optical transport network (backhaul). Multiple edge nodes, fanning out from the aggregation part of the network, have relatively lower capacity than switching nodes that are deeper into the backbone network, forming a distribution tree topology with high-capacity trunks at the base and lower capacity but with higher burstiness closer to the edge. The back-haul and mid-haul segments have steadier bandwidth due to the nature of statistical multiplexing of data streams. Thus, switches deep in the backbone network support the largest throughputs, but their switching speeds may be less demanding. Edge nodes need to switch faster to support the low latency requirements, but their capacities will be smaller. SDM in the optical domain, combined with WDM where needed for capacity, provides a single, highly flexible infrastructure that can concurrently support multiple heterogeneous streams of digital and/or analog radio over fiber (DRoF/ARoF, respectively) and is well suited for distributing heterogeneous traffic in a coordinated fashion through a converged infrastructure. Thus, space and spectrum resources are managed at the CO allowing an automated channel establishment between the CO and the cell sites in a 2-D space (WDM + SDM), pairing BBUs with RRUs. Management of the fronthaul network resources in a dynamic, adaptive, and energy-efficient way is suggested in [102].

The ODN is expected to be mainly passive, featuring low operating expenses and limited capital expenditure. By passive, we refer to a deployed fiber infrastructure utilizing multiplexers, splitters, and possibly filters with optional optical amplifiers to maintain a signal level. Different options are envisioned for the cell sites, as shown in the cell sites of Fig. 12(a)–(d). A first cell site option [Fig. 12(a)] is a purely spatially multiplexed site. The cell site transceivers are tuned to use the very same wavelength while using different cores either for scaling up the capacity or for implementing a dual-core duplex. As the cell site is programmed for single wavelength operation, this design allows for a common laser source to be shared among the transceivers for keeping the solution at low cost. Cell site options (b) and (c) correspond to spectrally multiplexed sites. Feeding the cell site is a single core while the multiplexing is exclusively performed in the wavelength domain. Cell site (b) features a passive device design, utilizing as an example an AWGR for separating and combining the wavelengths while keeping the implementation at low cost. An active device, such as a WSS, can be substituted, as shown in cell side (c), trading cost against flexibility. For spectrally multiplexed sites, dual-wavelength duplex is envisioned. Finally, a generic cell site option is depicted in Fig. 12(d) for full, reconfigurable flexibility. There, either spatial and/or wavelength multiplexing is used in order to use all the available network resources.

While we have noted the capacity enhancement and flexibility attribute of an SDM + WDM ODN, we need to further assess the choice of the SDM solution. Since the ODN establishes one-to-one connection pairs between BBU and RRU, the SDM solution cannot afford to be degraded by spatial channel mixing. This rules out MMF or coupled MCF SDM solutions. The ODN will be advantageously served by uncoupled MCF, over an SMF array, due to the greatly reduced timing skew feature of common cores in a single fiber cladding. The stochastic timing skew between cores or fibers, due to temperature fluctuations, is an order of magnitude larger for individual SMF than the intercore skew in the MCF, due to the strongly correlated environmental perturbations in the same MCF [103]. In a lab environment, over an 18-h testing period, the intercore skew remained below 4 ps, which is sufficiently low for exploitation of the spatial dimension in timing-critical applications, as a large bandwidth RF feeds to different antenna elements in a cell site. The impairments of AroF due to core crosstalk and Kerr nonlinearity have been investigated in [104] and found to be negligible.

The interconnection of mm-wave communications (tens of gigahertz carrier frequency), and all the more so THz-wave communications (hundreds of gigahertz [105]), affords significantly larger information bandwidths but is taxing the fronthaul segment between BBU and RRU with higher capacity requirements. Migration to AroF offers significant advantages over DroF [106]. By moving to analog transport, not only does AroF fronthaul maintain the centralization of the complete baseband processing, but also it further centralizes the digital-to-analog converter and analog-to-digital converter stages otherwise located at the antenna site. When combined with optical heterodyning, AroF becomes especially interesting for mm-wave and THz-wave signal generation. The CO sends both the analog information (converted from baseband to an intermediate frequency) and an offset carrier to the antenna site, where a fast photodiode performs the optical-to-electrical (O/E)

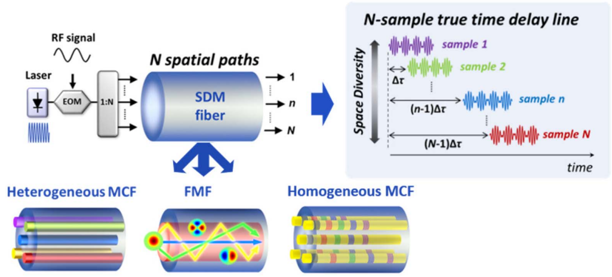

Fig. 13. ***Optical TTDL based on differential delays of guided modes within tailored SDM fibers. After [112].***

conversion and through optical heterodyning generates the RF signal at the desired carrier frequency (tens to hundreds of gigahertz), which is amplified toward the radiating antenna. The analog data and pilot tone can be sent on the same fiber or core, thereby maintaining their relative phase and polarization at the expense of frequency waste (due to the dead bandwidth between the two signals, which grows for higher center carrier frequencies). Alternatively, the pilot tone can be sent on a separate core (one or more cores for data streams and one core transporting the pilot tones), to be recombined at the receiver (with phase and polarization tracking potentially required) [107], [108]. An MCF can further be used in a multibeam antenna, where the beamformer network is kept at the CO and fed to the antenna on separate cores [109] and in power over fiber scenarios [110], [111].

SDM fibers can be tailored to operate as TTDLs, for applications such as optical beam steering for phased array antennas. Due to the unique guiding property of each mode (in MMF or heterogeneous MCF), the choice of mode and wavelength provides selectable constant delay samples (Fig. 13), as required for RF beam steering and other microwave photonics applications [112]. By engineering the design of MMF to achieve evenly spaced chromatic dispersion of the mode groups, continuously tunable TTDL can be dialed in by selecting the operating wavelength, which linearly scales the differential time delays between the modes [113]. This is achieved by optimizing the geometry of a double-cladding MMF design. The same optimization can be performed for heterogeneous MCF, tailoring the chromatic dispersion of each core by selecting its refractive index and core diameter and achieving evenly spaced dispersion [114].

The 5G/6G scenarios outlined above dealt with the distribution and beamforming of AroF feeding radiating antennas, yet some links benefit from direct FSO communications due to the highest available capacity of the optical channel. FSO links over several kilometer ranges offer robustness against electromagnetic interference, physical security due to very narrow, low divergence beams, and high-frequency reuse factors. However, the short wavelength carrier is susceptible to scattering and atmospheric turbulence. Traditionally, these are dealt with high power margins and adaptive optics mechanisms, hindering the uptake of FSO links. Adaptive optics requires sophisticated wavefront detection and modulation devices that can track the wavefront distortion evolution and remedy it. An alternative approach presented in [115] suggests directly coupling the distorted optical beam into a multimode fiber amplifier (in place a single-mode EDFA) followed by photodetection. The higher numerical aperture and diameter of the MMF allow the distorted wavefront to be efficiently coupled in, exciting proportionally higher order modes with greater atmospheric distortion. The received, spatially distorted optical signal undergoes amplification, which increases the photodetection sensitivity compared to the direct detection case that is thermal noise limited. This simple-to-implement scheme affords signal-ASE beat-noise-limited sensitivity for FSO links without any tracking or feedback controls.

VI. DATACENTER INTERCONNECTS AND NETWORKS

The current cloud infrastructure is based heavily on centralized architectures using network web-scale datacenters that host data repositories, services, and applications. These massive datacenters, each costing hundreds of millions of dollars, offer performance and economic benefits through the localized aggregation of resources and efficient management of power and heat.

As applications shift into the cloud, the data processing, storage, and transport requirements are growing rapidly. Traffic growth of 70% per year has been reported by Google [116] as well as from YouTube uploads and similar growth rates in Internet traffic [44]. Cloud providers have also commented that internal data flows are growing faster than external user data flows.

While technology continues to improve in terms of processing and communication capacities, its annualized growth rates are substantially lower with server performance (FLOPS) growing at 30%–40% per annum at constant power [44], [117] and datacenter switch capacities growing at 40% per annum [118]. This disparity is leading to an increase in the size and number of datacenters installations around the globe. The cloud network can be considered to consist of two logical networks: one that interconnects the servers and datacenters and another that connects the datacenters to the end users.

The networks that interconnect these cloud datacenters exist at a variety of length scales. There are the intra-datacenter networks that interconnect the servers within a building or warehouse scale, which have length scales from a few meters to hundreds of meters, and with tens to hundreds of thousands of server endpoints. Intra-datacenter networks commonly follow a three-tier Clos topology architecture (also called fat-tree architecture), with top-of-rack (ToR) switches at the lower tier (electronically connected to the servers within the rack), aggregation switches in the middle tier, and spine switches in the top tier [see Fig. 14(a)]. These electronic data/packet switches are capable of routing packets and operating networking protocols and offer higher data packet capacities for higher switching tiers. The electronic-packet switching tiers are interconnected by point-to-point fiber-optic links of increasing capacity as ascending through the tiers. The Clos topology provides redundancy, resiliency, and efficiency under uniformly spread data loads, which is imposed by load balancing measures. A typical packet path inside the datacenter will have to ascend through several switch tiers, each multiplexing higher capacities, before descending through the same fabric toward the destination server. The data bits experience multiple electrical/optical conversions and electronic switch processing, leading to excess power consumption and stochastic packet delay times from router output port queues. The large number of interconnected switch ports across the different tiers and short fiber spans makes cost minimizing of the transceivers a top priority. This leads to low power margins for transmission, a few decibels to overcome connector losses, which hinders the introduction of all-optical switching in

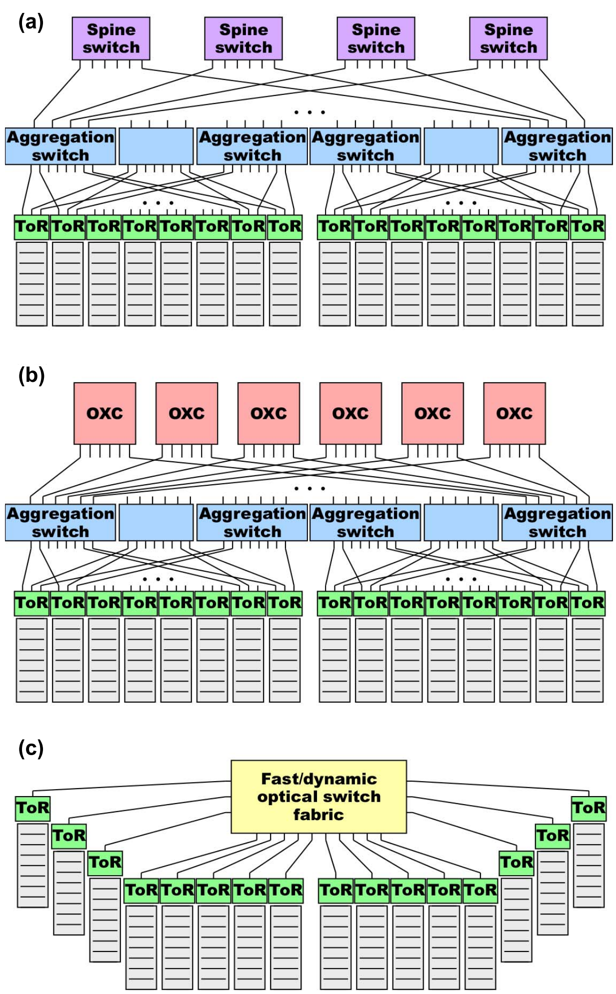

Fig. 14. *Intra-datacenter communications networks. (a) Fat-tree architecture, with tiered electronic switches and optical fiber links. (b) Replacement of top-tier data switches with slow optical circuit switches providing flexible direct connectivity between aggregation switches. (c) Flat optical layer, dynamically connecting ToR switches per demand.*

intra-datacenter applications, and thus, the interconnects serve as simple point-to-point links.

The prospects and challenges of all-optical switching for intra-datacenter applications, replacing the entire electronic fat-tree topology with a flat optical layer [Fig. 14(c)], are discussed in [119]. The main challenges for optical switching within the datacenter are the high dynamism with which servers exchange information, which can be met with electronic-packet networks. Optical switch fabrics are challenged by the required switching speeds and scheduling delays, often resorting to a hybrid approach separating short packet exchanges and long-lived flows [120]. An alternative to a flat optical layer topology has recently been disclosed by Google as operating within its datacenters, where the top-tier spline switches are being replaced by optical circuit switches [121] (implemented by low-loss, MEMS-based, OXC switches [122]). However, the functionality of spline switches and OXC are not interchangeable, requiring the datacenter to offset the lack of dynamic packet routing with traffic-engineered protocols (especially doing away with load balancing, instead seeking predictable capacity connectivity between aggregation switches that are served by long-lived, direct-connected links). By removing the spline switches and maintaining fixed connectivity matrices, the intra-datacenter network eliminates the additional stochastic delays and power draws and further facilitates incremental technology upgrades at the aggregation level (as transparent optical layer is oblivious to data rates and signaling format). Google reports that the optical layer undergoes reconfiguration at few days to weeks intervals, highlighting that the network copes with the unpredictability that occurs on short time scales.

There are also connections between datacenter sites within a region, or inter-datacenter, which are sufficiently physically separated to form an independent failure group or availability zone, having characteristic distances of few to tens of kilometers. These inter-datacenter links are mostly high-capacity trunks shuttling data between datacenters and providing redundancy and resiliency. These trunks deploy both WDM and SDM to maximize capacity, but no switching aspect presently. (Intermediate optical interconnects within buildings on a campus-sized site also exist, where connection distances may be up to 2 km, with traffic characteristics between inter- and intra-datacenter links.)

Finally, there are long-haul connections, hundreds of kilometers, and global-scale network connections, including thousands of kilometers undersea links that connect the global sites together. The network that connects to the end user consists of a global long-haul network, which provides connections to many points of presence where traffic can be delivered to metro and then fixed and wireless access networks. The technologies for both of these are discussed in Sections III-V. Initially, the networks for interconnecting the datacenters consisted of leased wavelengths from telecom carriers, but now due to the

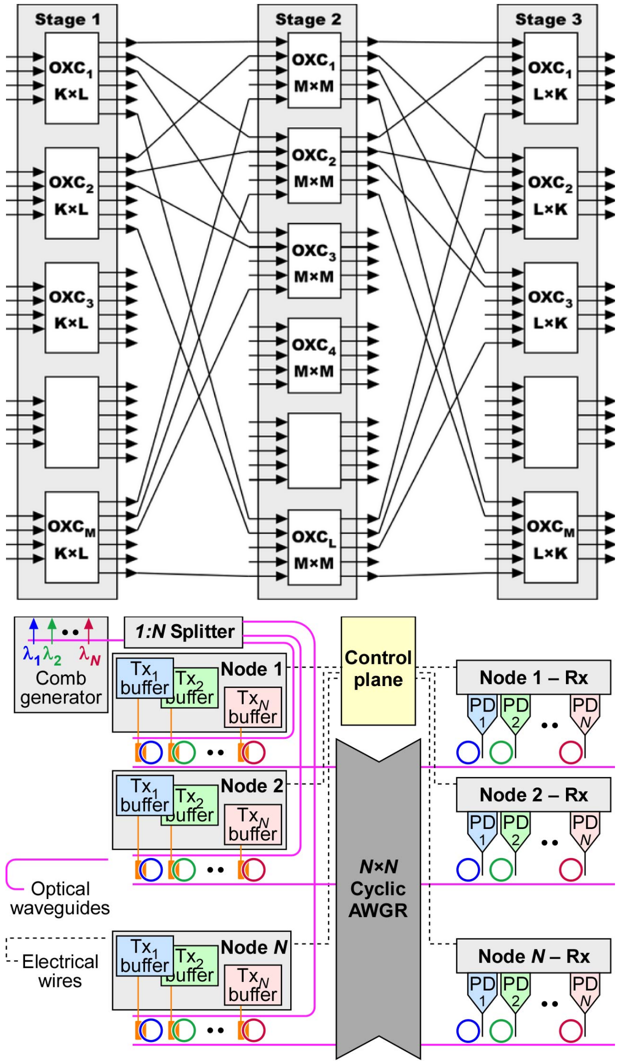

Fig. 15. ***Two classes of flat optical layer intra-datacenter connectivity. Top: full fiber switching at large scale with three-stage Benes architecture utilizing smaller OXC building blocks. Bottom: passive all-to-all connections by a cyclic AWGR with transmitter buffering and wavelength selection. From [119].***

experienced growth trends of these networks (50%–70% per year) [123], they are being built out exclusively by cloud companies with multiple fibers carrying the C + L band. They are also introducing features more important to them, such as SDN control planes and reconfigurability [124].

The interconnections within datacenters and between datacenter buildings have already embraced the use of massive spatial parallelism in the optical domain but at low spectral utilization. These interconnections are primarily based on using single wavelength (B&W) optical interconnects running at 25-Gb/s per fiber, with 50 and 100 Gb/s per fiber being introduced. The primary mechanism has been through increasing baud rates from 1 to 50 GBd with signaling formats being typically NRZ and PAM-4. Research work has demonstrated that serial modulation rates can be scaled higher, with 220-Gb/s OOK and 408-Gb/s 8-PAM [125]. Scaling to higher rates will likely introduce coherent detection technology to the datacenter [126]. Very large numbers (>10 000) of parallel SMFs are used for overall capacity in datacenters in the petabit per second scale. There is some limited use of coarse WDM (CWDM) where four or eight wavelengths are used to increase the per-fiber capacity. With increasing challenges in scaling baud rate, we expect these links to transition to using more wavelengths and to move to coherent communication approaches. Offering an optically switched environment at the scale required for datacenters (many thousands over complete fiber bandwidth), i.e., the flat topology of Fig. 14(c), can be addressed via an optical switch fabric consisting of multiple OXC placed in a Benes network [43] [Fig. 15 (top)]. While the Benes architecture can expand the switch scale, the realistic switching speed requirements for datacenter applications are still orders of magnitude faster than currently available in OXC. Alternative switching solutions that attempt to meet the scale and dynamism of the intra-datacenter environment are based on a passive all-to-all interconnection network based on cyclic $N \times N$ AWGR and fast tunable lasers [Fig. 15 (bottom)]. Here, data are buffered at the transmitter and launched to the desired receiver by wavelength selection. This optically accessed passively routed network is carried over SMF and is bandwidth-limited due to the AWGR's inherent filtering. The AWGR's port count can be increased by cascading smaller ones with differing free spectral ranges [127]. The space switching of the OXC and the wavelength routing of the AWGR represent two approaches for reconfiguring the datacenter network. Additional flexible resources can be utilized for networking, such as frequency [128], time slots [129], cores of MCF [130], and modes of MMF [131]. Alternatives to fiber resource switching approaches, such as free-space optics links employing beam steering mechanisms,are also being explored [132].

Links between datacenter sites are often implemented using very large numbers of fibers (hundreds to thousands) again using B&W or CWDM optical links. Pluggable coherent modules, such as 400ZR [133] which provides a digital coherent 400-Gb/s interface for 120 km or less, amplified, point-to-point, dense WDM noise limited links and unamplified, single wavelength, and loss limited links, are becoming available and cost competitive and are being extended to longer distances though 400ZR+ [134]. This is leading to the use of coherent transmission in B&W links. Since coherent modules already provide tunable and tightly controlled wavelengths, we expect a future transition of these links to using optical amplifiers and WDM for capacity scaling. While these links may end up looking like long-haul links with massive spatial parallelism and high spectral efficiency, it will represent a convergency from differing starting points.

VII. CONCLUSION

Societal intake of information has been rising exponentially for decades and will continue to do so for the foreseeable future. Serving this demand and scaling the transported capacity across all communication forms in a technology and cost-effective manner is a constant challenge the research community faces. As technology innovations are introduced into communication systems, demand is initially easily satisfied, but as it is rising exponentially, eventually inherent limits are reached. This is currently the state of affairs in fiber-optic communications, where the capacity limits of SMF are well understood and rapidly approaching.

In this article, we addressed the prospects of the next generation of optical fibers making use of SDM and ancillary components to address the inherent limitation of SMF. We analyzed the four essential communication sectors of terrestrial, undersea, wireless, and datacenters, which represent the entire communication chain. In each communication scenario, we find not only that SDM fiber and components can potentially offer capacity scale but also some technical advantages alongside new, inevitable challenges that can be addressed by clever engineering. The adoption of spatial and spectral multiplexing (SDM + WDM) necessitates new optical switch developments and optical node architectures to effectively manage and route traffic in such networks. Initial utilization of SDM technology in communication systems is commencing, in capacity-saturated terrestrial links, in undersea systems using parallel SMF fibers due to electrical power delivery limitations, and in datacenter interconnect cables due to low-power budgets. We highlighted the potential of further benefits of SDM + WDM optical networks, which may be incorporated in the future. However, as we are in the dawn of a new era, it is impossible to predict how the technology will evolve. We hope that this article will stimulate new ideas and enterprises among its readers. ■

Acknowledgment

The assistance of Ph.D. student Charalampos Papapavlou in the preparation of some figures is acknowledged.

REFERENCES

[1] M. Roser, H. Ritchie, and E. Ortiz-Ospina. (2015). *Internet*. [Online]. Available: https://ourworldindata.org/internet
[2] M. Vallo and P. Mukish, "Global insights into the key technology enabling the exponential growth of digital communication networks," in *Proc. SPIE, Metro Data Center Opt. Netw. Short-Reach Links IV*, vol. 11712, 2015, pp. 1–6, Paper 117120F.
[3] A. D. Ellis, J. Zhao, and D. Cotter, "Approaching the non-linear Shannon limit," *J. Lightw. Technol.*, vol. 28, no. 4, pp. 423–433, Feb. 15, 2010.
[4] R. Essiambre, G. Kramer, P. J. Winzer, G. J. Foschini, and B. Goebel, "Capacity limits of optical fiber networks," *J. Lightw. Technol.*, vol. 28, no. 4, pp. 662–701, Feb. 15, 2010.
[5] T. Morioka, "New generation optical infrastructure technologies: EXAT initiative towards 2020 and beyond," in *Proc. 14th Optoelectron. Commun. Conf. (OECC)*, Jul. 2009, pp. 1–2, Paper FT4.
[6] P. J. Winzer, "Energy-efficient optical transport capacity scaling through spatial multiplexing," *IEEE Photon. Technol. Lett.*, vol. 23, no. 13, pp. 851–853, Jul. 1, 2011.
[7] D. Richardson, J. Fini, and L. Nelson, "Space-division multiplexing in optical fibres," *Nature Photon.*, vol. 7, no. 5, pp. 354–362, 2013.
[8] D. M. Marom et al., "Survey of photonic switching architectures and technologies in support of spatially and spectrally flexible optical networking," *J. Opt. Commun. Netw.*, vol. 9,

pp. 1–26, Jan. 2017.
[9] B. J. Puttnam, G. Rademacher, and R. S. Luís, "Space-division multiplexing for optical fiber communications," *Optica*, vol. 8, pp. 1186–1203, Sep. 2021.
[10] T. Hayashi, Y. Tamura, T. Hasegawa, and T. Taru, "Record-low spatial mode dispersion and ultra-low loss coupled multi-core fiber for ultra-long-haul transmission," *J. Lightw. Technol.*, vol. 35, no. 3, pp. 450–457, Feb. 1, 2017.
[11] T. Hayashi et al., "Coupled-core multi-core fibers: High-spatial-density optical transmission fibers with low differential modal properties," in *Proc. Eur. Conf. Opt. Commun. (ECOC)*, Sep. 2015, pp. 1–3.
[12] T. Mizuno et al., "Long-haul dense space-division multiplexed transmission over low-crosstalk heterogeneous 32-core transmission line using a partial recirculating loop system," *J. Lightw. Technol.*, vol. 35, no. 3, pp. 488–498, Feb. 1, 2017.
[13] G. Milione et al., "Mode crosstalk matrix measurement of a 1 km elliptical core few-mode optical fiber," *Opt. Lett.*, vol. 41, pp. 2755–2758, Jun. 2016.
[14] A. Corsi, J. H. Chang, L. A. Rusch, and S. LaRochelle, "Design of highly elliptical core ten-mode fiber for space division multiplexing with 2 × 2 MIMO," *IEEE Photon. J.*, vol. 11, no. 2, pp. 1–10, Apr. 2019.
[15] M. Takahashi et al., "Uncoupled 4-core fibre with ultra-low loss and low inter core crosstalk," in *Proc. Eur. Conf. Opt. Commun. (ECOC)*, 2020, pp. 1–4, Paper Th1A-5.
[16] D. Soma et al., "10.16-Peta-B/s dense SDM/WDM transmission over 6-mode 19-core fiber across the C+L band," *J. Lightw. Technol.*, vol. 36, no. 6, pp. 1362–1368, Mar. 2018.
[17] B. J. Puttnam et al., "1 Pb/s transmission in a 125 μm diameter 4-core MCF," in *Proc. Conf. Lasers Electro-Opt. (CLEO)*, 2022, pp. 1–2, Paper JTh6B.1.
[18] G. Rademacher et al., "Peta-bit-per-second optical communications system using a standard cladding diameter 15-mode fiber," *Nature Commun.*, vol. 12, no. 1, p. 4238, Dec. 2021.
[19] M. D. Feuer et al., "Joint digital signal processing receivers for spatial superchannels," *IEEE Photon. Technol. Lett.*, vol. 24, no. 21, pp. 1957–1960, Nov. 1, 2012.
[20] Y. Jung, J. R. Hayes, S. U. Alam, and D. J. Richardson, "Multicore fibre fan-in/fan-out device using fibre optic collimators," in *Proc. Eur. Conf. Opt. Commun. (ECOC)*, Sep. 2017, pp. 1–3.
[21] V. I. Kopp, J. Park, M. Wlodawski, J. Singer, D. Neugroschl, and A. Z. Genack, "Pitch reducing optical fiber array and multicore fiber for space-division multiplexing," in *Proc. IEEE Photon. Soc. Summer Topical Meeting*, Jul. 2013, pp. 99–100.
[22] W. Ji et al., "Spacing-tailored multicore fiber interface for efficient FIFO devices," *J. Lightw. Technol.*, vol. 40, no. 16, pp. 5682–5688, Aug. 15, 2022, doi: 10.1109/JLT.2022.3177622.
[23] R. R. Thomson et al., "Ultrafast-laser inscription of a three-dimensional fan-out device for multicore fiber coupling applications," *Opt. Exp.*, vol. 15, pp. 11691–11697, Sep. 2007.
[24] Y. Ding et al., "On-chip grating coupler array on the SOI platform for fan-in/fan-out of MCFs with low insertion loss and crosstalk," *Opt. Exp.*, vol. 23, pp. 3292–3298, Sep. 2015.
[25] A. Andrusier, M. Shtaif, C. Antonelli, and A. Mecozzi, "Assessing the effects of mode-dependent loss in space-division multiplexed systems," *J. Lightw. Technol.*, vol. 32, no. 7, pp. 1317–1322, Apr. 2014.
[26] S. G. Leon-Saval, A. Argyros, and J. Bland-Hawthorn, "Photonic lanterns," *Nanophotonics*, vol. 2, nos. 5–6, pp. 429–440, Dec. 2013.
[27] G. Labroille et al., "Efficient and mode selective spatial mode multiplexer based on multi-plane light conversion," *Opt. Exp.*, vol. 22, pp. 15599–15607, Jun. 2014.
[28] T. Fujisawa et al., "Scrambling-type three-mode PLC multiplexer based on cascaded Y-branch waveguide with integrated mode rotator," *J. Lightw. Technol.*, vol. 36, no. 10, pp. 1985–1992, May 15, 2018.
[29] Y. Ma, L. Stewart, J. Armstrong, I. G. Clarke, and G. Baxter, "Recent progress of wavelength selective switch," *J. Lightw. Technol.*, vol. 39, no. 4, pp. 896–903, Feb. 15, 2021.
[30] R. Spanke, "Architectures for large nonblocking optical space switches," *IEEE J. Quantum Electron.*, vol. JQE-22, no. 6, pp. 964–967, Jun. 1986.
[31] S. Frisken, G. Baxter, D. Abakoumov, H. Zhou, I. Clarke, and S. Poole, "Flexible and grid-less wavelength selective switch using LCOS technology," in *Proc. Opt. Fiber Commun. Conf. Nat. Fiber Opt. Eng. Conf. (OFC/NFOEC)*, 2011, pp. 1–3, Paper OTuM3.
[32] T. J. Seok et al., "Silicon photonic wavelength cross-connect with integrated MEMS switching," *APL Photon.*, vol. 4, no. 10, Oct. 2019, Art. no. 100803.
[33] K. Prifti, A. Gasser, N. Tessema, X. Xue, R. Stabile, and N. Calabretta, "System performance evaluation of a nanoseconds modular photonic integrated WDM WSS for optical data center networks," in *Proc. Opt. Fiber Commun. Conf. (OFC)*, 2019, pp. 1–3, Paper Th2A.31.
[34] N. K. Fontaine, M. Mazur, R. Ryf, H. Chen, L. Dallachiesa, and D. T. Neilson, "36-THz bandwidth wavelength selective switch," in *Proc. Eur. Conf. Opt. Commun. (ECOC)*, Sep. 2021, pp. 1–4, Paper PD2.3.
[35] R. Kraemer et al., "Multi-band photonic integrated wavelength selective switch," *J. Lightw. Technol.*, vol. 39, no. 19, pp. 6023–6032, Oct. 1, 2021.
[36] K. Suzuki et al., "Wavelength selective switch for multi-core fiber based space division multiplexed network with core-by-core switching capability," in *Proc. 21st Optoelectron. Commun. Conf. (OECC)*, 2016, pp. 1–2, Paper WF1-2.
[37] H. Yang et al., "24 [1×12] wavelength selective switches integrated on a single 4k LCoS device," *J. Lightw. Technol.*, vol. 39, no. 4, pp. 1033–1039, Feb. 15, 2021.
[38] L. E. Nelson et al., "Spatial superchannel routing in a two-span ROADM system for space division multiplexing," *J. Lightw. Technol.*, vol. 32, no. 4, pp. 783–789, Feb. 2014.
[39] D. M. Marom et al., "Wavelength-selective switch with direct few mode fiber integration," *Opt. Exp.*, vol. 23, no. 5, pp. 5723–5737, 2015.
[40] H. Chen et al., "Wavelength selective switch for commercial multimode fiber supporting 576 spatial channels," in *Proc. Eur. Conf. Opt. Commun. (ECOC)*, 2016, pp. 1–3.
[41] M. Jinno, I. Urashima, T. Ishikawa, T. Kodama, and Y. Uchida, "Core selective switch with low insertion loss over ultra-wide wavelength range for spatial channel networks," *J. Lightw. Technol.*, vol. 40, no. 6, pp. 1821–1828, Mar. 15, 2022.
[42] A. C. Jatoba-Neto et al., "Scaling SDM optical networks using full-spectrum spatial switching," *J. Opt. Commun. Netw.*, vol. 10, no. 12, pp. 991–1004, 2018.
[43] D. M. Marom, R. Ryf, and T. D. Neilson, "Networking and routing in space-division multiplexed systems," in *Optical Fiber Telecommunications VII*, A. E. Willner, Ed. New York, NY, USA: Academic, 2020.
[44] P. J. Winzer and D. T. Neilson, "From scaling disparities to integrated parallelism: A decathlon for a decade," *J. Lightw. Technol.*, vol. 35, no. 5, pp. 1099–1115, Mar. 2017.
[45] J. Kim et al., "1100×1100 port MEMS-based optical crossconnect with 4-dB maximum loss," *IEEE Photon. Technol. Lett.*, vol. 15, no. 11, pp. 1537–1539, Nov. 2003.
[46] X. Zheng et al., "Three-dimensional MEMS photonic cross-connect switch design and performance," *IEEE J. Sel. Topics Quantum Electron.*, vol. 9, no. 2, pp. 571–578, Mar./Apr. 2003.
[47] T. J. Seok, K. Kwon, J. Henriksson, J. Luo, and M. C. Wu, "Wafer-scale silicon photonic switches beyond die size limit," *Optica*, vol. 6, no. 4, pp. 490–494, Apr. 2019.
[48] H. C. H. Mulvad et al., "Beam-steering all-optical switch for multi-core fibers," in *Proc. Opt. Fiber Commun. Conf. (OFC)*, 2017, pp. 1–3, Paper Tu2C.4.
[49] C. Deakin, M. Enrico, N. Parsons, and G. Zervas, "Design and analysis of beam steering multicore fiber optical switches," *J. Lightw. Technol.*, vol. 37, no. 9, pp. 1954–1963, May 1, 2019.
[50] L. Rapp and M. Eiselt, "Optical amplifiers for multi–band optical transmission systems," *J. Lightw. Technol.*, vol. 40, no. 6, pp. 1579–1589, Mar. 15, 2022.
[51] A. Ferrari et al., "Assessment on the achievable throughput of multi-band ITU-T G.652.D fiber transmission systems," *J. Lightw. Technol.*, vol. 38, no. 16, pp. 4279–4291, Aug. 15, 2020.
[52] A. H. Gnauck et al., "Efficient pumping scheme for amplifier arrays with shared pump laser," in *Proc. 42nd Eur. Conf. Opt. Commun. (ECOC)*, 2016, pp. 1–3.
[53] S. Jain et al., "32-core erbium/ytterbium-doped multicore fiber amplifier for next generation space-division multiplexed transmission system," *Opt. Exp.*, vol. 25, no. 26, pp. 32887–32896, 2017.
[54] E. Ip et al., "146λ×6×19-Gbaud wavelength-and mode-division multiplexed transmission over 10×50-km spans of few-mode fiber with a gain-equalized few-mode EDFA," *J. Lightwave Technol.*, vol. 32, no. 4, pp. 790–797, 2013.
[55] M. Moralis-Pegios et al., "4-channel 200 Gb/s WDM O-band silicon photonic transceiver sub-assembly," *Opt. Exp.*, vol. 28, no. 4, pp. 5706–5714, Feb. 2020.
[56] D. Kong et al., "Intra-datacenter interconnects with a serialized silicon optical frequency comb modulator," *J. Lightw. Technol.*, vol. 38, no. 17, pp. 4677–4682, Sep. 1, 2020.
[57] S. Fathololoumi et al., "1.6 Tbps silicon photonics integrated circuit and 800 Gbps photonic engine for switch co-packaging demonstration," *J. Lightw. Technol.*, vol. 39, no. 4, pp. 1155–1161, Feb. 15, 2021.
[58] J. Du et al., "High speed and small footprint silicon micro-ring modulator assembly for space-division-multiplexed 100-Gbps optical interconnection," *Opt. Exp.*, vol. 26, no. 11, pp. 13721–13729, 2018.
[59] T. Kobayashi et al., "1-Pb/s (32 SDM/46 WDM/768 Gb/s) C-band dense SDM transmission over 205.6-km of single-mode heterogeneous multi-core fiber using 96-Gbaud PDM-16QAM channels," in *Proc. Opt. Fiber Commun. Conf. (OFC)*, 2017, pp. 1–3, Paper Th5B.1.
[60] T. Sakamoto et al., "Low-loss and low-DMD few-mode multi-core fiber with highest core multiplicity factor," in *Proc. Opt. Fiber Commun. Conf. (OFC)*, 2016, pp. 1–3, Paper Th5A.2.
[61] K. Pulverer et al., "First demonstration of single-mode MCF transport network with crosstalk-aware in-service optical channel control," in *Proc. Eur. Conf. Opt. Commun. (ECOC)*, 2017, pp. 1–3, Paper PDP4.
[62] S. Takasaka et al., "Increase of cladding pump power efficiency by a 19-core erbium doped fibre amplifier," in *Proc. Eur. Conf. Opt. Commun. (ECOC)*, 2017, pp. 1–3, Paper Th.2.D.3.
[63] J. Thouras, E. Pincemin, D. Amar, P. Gravey, M. Morvan, and M.-L. Moulinard, "Introduction of 12 cores optical amplifiers in optical transport network: Performance study and economic impact," in *Proc. 20th Int. Conf. Transparent Opt. Netw. (ICTON)*, 2018, pp. 1–4, Paper We.C2.4.
[64] M. Wada et al., "Cladding pumped randomly coupled 12-core erbium-doped fiber amplifier with low mode-dependent gain," *J. Lightw. Technol.*, vol. 36, no. 5, pp. 1220–1225, Mar. 1, 2018.
[65] H. Ono, Y. Miyamoto, T. Mizuno, and M. Yamada, "Gain control in multi-core erbium-doped fiber amplifier with cladding and core hybrid pumping," *J. Lightw. Technol.*, vol. 37, no. 13, pp. 3365–3372, Jul. 1, 2019.
[66] E. Le Taillandier de Gabory, K. Matsumoto, S. Fujita, S. Nakamura, S. Yanagimachi, and J. Abe, "Transmission of 256 Gb/s PM-16 QAM signal through hybrid cladding and core pumping scheme MC-EDFA controlled for reduced power consumption," in *Proc. Opt. Fiber Commun. Conf.*

(OFC), 2017, pp. 1–3, Paper Th1C1.
[67] T. Matsui et al., "118.5 Tbit/s transmission over 316 km-long multi-core fiber with standard cladding diameter," in *Proc. Opto-Electron. Commun. Conf. (OECC) Photon. Global Conf. (PGC)*, 2017, pp. 1–2.
[68] K. Yonenaga et al., "Demonstration of 10-Tbit/s multi-granularity optical cross-connect node toward 100-Tbit/s scalability," in *Proc. Opt. Fiber Commun. Conf. (OFC)*, 2009, pp. 1–3, Paper PDP-C4.
[69] R. Yang, L. Liu, S. Yan, and D. Simeonidou, "A programmable ROADM system for SDM/WDM networks," *Appl. Sci.*, vol. 11, no. 9, p. 4195, May 2021.
[70] T. Kuno, Y. Mori, S. Subramaniam, M. Jinno, and H. Hasegawa, "Design and evaluation of a reconfigurable optical add-drop multiplexer with flexible wave-band routing in SDM networks," *J. Opt. Commun. Netw.*, vol. 14, no. 4, p. 248, 2022.
[71] R. Schmogrow, "Solving for scalability from multi-band to multi-rail core networks," *J. Lightw. Technol.*, vol. 40, no. 11, pp. 3406–3414, Jun. 1, 2022.
[72] M. Jinno and T. Kodama, "Spatial channel network (SCN): Introducing spatial bypass toward the SDM era," in *Proc. Opt. Fiber Commun. Conf. (OFC)*, 2020, pp. 1–3, Paper M2G.1.
[73] R. S. Luis et al., "Demonstration of a 1 Pb/s spatial channel network node," in *Proc. 45th Eur. Conf. Opt. Commun. (ECOC)*, 2019, pp. 1–4, Paper PD.3.5.
[74] D. M. Marom and M. Blau, "Switching solutions for WDM-SDM optical networks," *IEEE Commun. Mag.*, vol. 53, no. 2, pp. 60–68, Feb. 2015.
[75] Y. Miyamoto, K. Suzuki, and K. Nakajima, "Multicore fiber transmission system for high-capacity optical transport network," in *Proc. SPIE, Next-Gener. Opt. Commun., Compon., Sub-Syst., Syst. VIII*, vol. 10947, 2019, pp. 1–11, Paper 1094703.
[76] Y. Tanaka, H. Hasegawa, and K. Sato, "Criteria for selecting subsystem configuration in creating large-scale OXCs," *J. Opt. Commun. Netw.*, vol. 7, pp. 1009–1017, Oct. 2015.
[77] K. Suzuki, K. Seno, and Y. Ikuma, "Application of waveguide/free-space optics hybrid to ROADM device," *J. Lightw. Technol.*, vol. 35, no. 4, pp. 596–606, Feb. 15, 2017.
[78] K. Yamaguchi et al., "Integrated wavelength selective switch array for space division multiplexed network with ultra-low inter-spatial channel crosstalk," in *Proc. Opt. Fiber Commun. Conf. (OFC)*, 2018, pp. 1–3, Paper Th1J.3.
[79] K. Seno, N. Nemoto, and Y. Miyamoto, "Wavelength selective switches for SDM photonic nodes based on SPOC platform," in *Proc. Opt. Fiber Commun. Conf. (OFC)*, 2021, pp. 1–3, Paper W1A.5.
[80] K. Seno, N. Nemoto, K. Yamaguchi, M. Nakajima, K. Suzuki, and Y. Miyamoto, "Wavelength selective devices for SDM applications based on SPOC platform," *J. Lightw. Technol.*, vol. 40, no. 6, pp. 1764–1775, Mar. 15, 2022.
[81] H. Takeshita, M. Sato, and Y. Inada, "Past, current and future technologies for optical submarine cable," in *Proc. IEEE/ACM Workshop Photon. Opt. Technol. Oriented Netw., Inf. Comput. Syst. (PHOTONICS)*, 2019, pp. 36–42.
[82] C. Papapavlou, K. Paximadis, D. Uzunidis, and I. Tomkos, "Toward SDM-based submarine optical networks: A review of their evolution and upcoming trends," *Telecom*, vol. 3, no. 2, pp. 234–280, Apr. 2022.
[83] "Will multiband or/and multidimensional, SDM effectively address the need for increased network capacity?" in *Proc. Opt. Fiber Commun. (OFC) Conf.*, Jun. 2021.
[84] K. Paximadis and C. Papapavlou, "Towards an all new submarine optical network for the Mediterranean Sea: Trends, design and economics," in *Proc. 12th Int. Conf. Netw. Future (NoF)*, 2021, pp. 1–5.
[85] C. Papapavlou, K. Paximadis, and G. Tzimas, "Design and analysis of a new SDM submarine optical network for Greece," in *Proc. 12th Int. Conf. Inf., Intell., Syst. Appl. (IISA)*, 2021, pp. 1–8.
[86] T. Frishch and S. Desbruslais, "Electrical power, a potential limit to cable capacity," in *Proc. SubOptic*, 2013, pp. 1–5, Paper TUIC-04.
[87] A. Pilipetskii, "High capacity submarine transmission systems," in *Proc. Opt. Fiber Commun. Conf. (OFC)*, 2015, pp. 1–3, Paper W3G.5.
[88] C. Ciauri. *The Dunant Subsea Cable, Connecting the U.S. and Mainland Europe, Is Ready for Service*. Accessed: May 1, 2022. [Online]. Available: https://cloud.google.com/blog/products/infrastructure/googles-dunant-subsea-cable-is-now-ready-for-service
[89] J. D. Downie, X. Liang, and S. Makovejs, "Assessing capacity and cost/capacity of 4-core multicore fibers against single core fibers in submarine cable systems," *J. Lightwave Technol.*, vol. 38, no. 11, pp. 3015–3022, Mar. 16, 2020.
[90] J. D. Downie, X. Liang, and S. Makovejs, "Modeling the techno-economics of multicore optical fibers in subsea transmission systems," *J. Lightw. Technol.*, vol. 40, no. 6, pp. 1569–1578, Mar. 15, 2022.
[91] S. Beppu et al., "Real-time transoceanic coupled 4-core fiber transmission," in *Proc. Opt. Fiber Commun. Conf. (OFC)*, 2021, pp. 1–3, Paper F3B.4.
[92] P. Pecci et al., "Pump farming as enabling factor to increase subsea cable," in *Proc. SubOptic*, 2019, pp. 1–7, Paper OP14-4.
[93] E. Le Taillandier de Gabory, "Low power consumption optical amplification using multicore erbium doped fiber amplifiers," in *Proc. IEEE Photon. Soc.*, 2018. [Online]. Available: https://perso.telecom-paristech.fr/gallion/ieee-photonics/IEEE_FrenchChapter_20180611_ELTdG_Released.pdf
[94] L. D. Garrett, "Design of global submarine networks [Invited]," *J. Opt. Commun. Netw.*, vol. 10, no. 2, pp. A185–A195, 2018.
[95] S. Wong. *Google's Subsea Fiber Optics, Explained*. Accessed: May 1, 2022. [Online]. Available: https://cloud.google.com/blog/topics/developers-practitioners/googles-subsea-fiber-optics-explained
[96] *TE SubCom and Nistica Announce Availability of Undersea Qualified Wavelength Selective Switch Modules*. Accessed: May 1, 2022. [Online]. Available: https://www.subcableworld.com/newsfeed/technology/te-subcom-and-nistica-announce-availability-of-undersea-qualified-wavelength-selective-switch-modules
[97] T. A. Strasser and J. L. Wagener, "Wavelength-selective switches for ROADM applications," *IEEE J. Sel. Topics Quantum Electron.*, vol. 16, no. 5, pp. 1150–1157, Sep./Oct. 2010.
[98] *IMT Traffic Estimates for the Years 2020 to 2030*, document Rep. ITU-R M.2370-0, 2015. [Online]. Available: https://www.itu.int/pub/R-REP-M.2370-2015
[99] L. Bariah et al., "A prospective look: Key enabling technologies, applications and open research topics in 6G networks," *IEEE Access*, vol. 8, pp. 174792–174820, 2020.
[100] M. Xiao et al., "Millimeter wave communications for future mobile networks," *IEEE J. Sel. Areas Commun.*, vol. 35, no. 9, pp. 1909–1935, Sep. 2017.
[101] S. Rommel, D. Perez-Galacho, J. M. Fabrega, R. Munoz, S. Sales, and I. T. Monroy, "High-capacity 5G fronthaul networks based on optical space division multiplexing," *IEEE Trans. Broadcast.*, vol. 65, no. 2, pp. 434–443, Jun. 2019.
[102] T. Lagkas, D. Klonidis, P. Sarigiannidis, and I. Tomkos, "Optimized joint allocation of radio, optical, and MEC resources for the 5G and beyond fronthaul," *IEEE Trans. Netw. Service Manage.*, vol. 18, no. 4, pp. 4639–4653, Dec. 2021.
[103] W. Klaus et al., "Advanced space division multiplexing technologies for optical networks," *J. Opt. Commun. Netw.*, vol. 9, no. 4, p. C1, 2017.
[104] A. Macho, M. Morant, and R. Llorente, "Next-generation optical fronthaul systems using multicore fiber media," *J. Lightw. Technol.*, vol. 34, no. 20, pp. 4819–4827, Oct. 15, 2016.
[105] A.-A. A. Boulogeorgos et al., "Terahertz technologies to deliver optical network quality of experience in wireless systems beyond 5G," *IEEE Commun. Mag.*, vol. 56, no. 6, pp. 144–151, Jun. 2018.
[106] S. Rommel et al., "Towards a scaleable 5G fronthaul: Analog radio-over-fiber and space division multiplexing," *J. Lightw. Technol.*, vol. 38, no. 19, pp. 5412–5422, Oct. 1, 2020.
[107] B. J. Puttnam et al., "High-capacity self-homodyne PDM-WDM-SDM transmission in a 19-core fiber," *Opt. Exp.*, vol. 22, no. 18, pp. 21185–21191, Sep. 2014.
[108] B. Puttnam et al., "Self-homodyne detection in optical communication systems," *Photonics*, vol. 1, no. 2, pp. 110–130, May 2014.
[109] M. Morant, A. Trinidad, E. Tangdiongga, T. Koonen, and R. Llorente, "Experimental demonstration of mm-wave 5G NR photonic beamforming based on ORRs and multicore fiber," *IEEE Trans. Microw. Theory Techn.*, vol. 67, no. 7, pp. 2928–2935, Jul. 2019.
[110] C. Vazquez et al., "Multicore fiber scenarios supporting power over fiber in radio over fiber systems," *IEEE Access*, vol. 7, pp. 158409–158418, 2019.
[111] J. D. López-Cardona et al., "Power-over-fiber in a 10 km long multicore fiber link within a 5G fronthaul scenario," *Opt. Lett.*, vol. 46, pp. 5348–5351, Nov. 2021.
[112] M. Ureña et al., "Specialty fibers exploiting spatial multiplexing for signal processing in radio access networks," in *Proc. Int. Conf. Opt. Netw. Design Modeling (ONDM)*, 2021, pp. 1–3.
[113] E. Nazemosadat and I. Gasulla, "Dispersion-tailored few-mode fiber design for tunable microwave photonic signal processing," *Opt. Exp.*, vol. 28, no. 24, pp. 37015–37025, 2020.
[114] S. García, M. Ureña, and I. Gasulla, "Demonstration of distributed radiofrequency signal processing on heterogeneous multicore fibres," in *Proc. 45th Eur. Conf. Opt. Commun. (ECOC)*, 2019, pp. 1–4.
[115] H. Liu et al., "Turbulence-resistant FSO communication using a few-mode pre-amplified receiver," *Sci. Rep.*, vol. 9, no. 1, p. 16247, Dec. 2019.
[116] A. Singh et al., "Jupiter rising: A decade of clos topologies and centralized control in Google's datacenter network," in *Proc. ACM Conf. Special Interest Group Data Commun. (SIGCOMM)*, 2015, pp. 183–197.
[117] K. Rupp. *CPU, GPU and MIC Hardware Characteristics Over Time*. [Online]. Available: https://www.karlrupp.net/2013/06/cpu-gpu-and-mic-hardware-characteristics-over-time/
[118] R. J. Stone, "Use of embedded optics to decrease power consumption in IO dense systems," in *Proc. Opt. Fiber Commun. Conf. (OFC)*, 2017, pp. 1–3.
[119] S. J. Ben Yoo, "Prospects and challenges of photonic switching in data centers and computing systems," *J. Lightw. Technol.*, vol. 40, no. 8, pp. 2214–2243, Apr. 15, 2022.
[120] J. Perelló et al., "All-optical packet/circuit switching-based data center network for enhanced scalability, latency, and throughput," *IEEE Netw.*, vol. 27, no. 6, pp. 14–22, Nov. 2013.
[121] L. Poutievski et al., "Jupiter evolving: Transforming Google's datacenter network via optical circuit switches and software-defined networking," in *Proc. ACM SIGCOMM Conf.*, Aug. 2022, pp. 66–85.
[122] R. Urata et al., "Mission Apollo: Landing optical circuit switching at datacenter scale," 2022, *arXiv:2208.10041*.
[123] C.-Y. Hong et al., "B4 and after: Managing hierarchy, partitioning, and asymmetry for availability and scale in Google's software-defined WAN," in *Proc. Conf. ACM Special Interest Group Data Commun.*, Aug. 2018, pp. 74–87.
[124] A. Vahdat et al., "Orion: Google's software-defined networking control plane," in *Proc. Netw. Sys. Design Implement. (NSDI)*, 2021, pp. 83–98, 2021.
[125] M. Eppenberger et al., "Plasmonic racetrack modulator transmitting 220 Gbit/s OOK and 408

Gbit/s 8PAM," in *Proc. Eur. Conf. Opt. Commun. (ECOC)*, 2021, pp. 1–4.
[126] X. Zhou, R. Urata, and H. Liu, "Beyond 1 Tb/s intra-data center interconnect technology: IM-DD OR coherent?" *J. Lightw. Technol.*, vol. 38, no. 2, pp. 475–484, Jan. 15, 2020.
[127] T. Niwa, H. Hasegawa, K. Sato, T. Watanabe, and H. Takahashi, "Large port count wavelength routing optical switch consisting of cascaded small-size cyclic arrayed waveguide gratings," *IEEE Photon. Technol. Lett.*, vol. 24, no. 22, pp. 2027–2030, Nov. 2012.
[128] P. N. Ji et al., "Design and evaluation of a flexible-bandwidth OFDM-based intra-data center interconnect," *J. Sel. Top. Quantum Electron.*, vol. 19, no. 2, 2013, Art. no. 3700310.
[129] K. Kondepu et al., "Fully SDN-enabled all-optical architecture for data center virtualization with time and space multiplexing," *J. Opt. Commun. Netw.*, vol. 10, no. 7, pp. B90–B101, Jul. 2018.
[130] H. Yuan, M. Furdek, A. Muhammad, A. Saljoghei, L. Wosinska, and G. Zervas, "Space-division multiplexing in data center networks: On multi-core fiber solutions and crosstalk-suppressed resource allocation," *IEEE/OSA J. Opt. Commun. Netw.*, vol. 10, no. 4, pp. 272–288, Apr. 2018.
[131] S. Guo, S. Yin, R. Ma, B. Wang, and S. Huang, "Crosstalk-aware routing, spectrum, mode and time assignment using FMF with partial MIMO equalization in flexible grid datacenter networks," *Opt. Commun.*, vol. 436, pp. 180–187, May 2019.
[132] C. Chaintoutis et al., "Free space intra-datacenter interconnects based on 2D optical beam steering enabled by photonic integrated circuits," *Photonics*, vol. 5, no. 3, p. 21, Sep. 2018.
[133] *OIF 400ZR*. Accessed: Dec. 12, 2021. [Online]. Available: https://www.oiforum.com/technical-work/hot-topics/400zr-2/
[134] *OpenZR+MSA*. [Online]. Available: https://openzrplus.org

ABOUT THE AUTHORS

Dan M. Marom (Senior Member, IEEE) received the Ph.D. degree in electrical engineering from the University of California at San Diego, La Jolla, CA, USA, in 2000, with a focus on instantaneous signal processing of ultrafast waveforms with nonlinear wave mixing.

He is currently a Professor and the Chair of the Department of Applied Physics, Hebrew University of Jerusalem, Jerusalem, Israel, where he heads the Photonic Devices Group. After his Ph.D. degree, he joined the Advanced Photonics Research Department, Bell Laboratories, Lucent Technologies, Holmdel, NJ, USA, as a Member of the Technical Staff, where he developed wavelength-selective switches and other filtering and switching components. Since 2005, he has been with the Hebrew University of Jerusalem. Over more than 20-year research career in optical communications, he has been involved in the development of various optical switches for telecommunications applications, utilizing free-space and guided-wave optics and different switching mechanisms, including micro-electromechanical systems, liquid crystals, and nonlinear media.

Prof. Marom is a Senior Member of the IEEE Photonics Society and a Fellow of the Optical Society of America. He was awarded the IEEE Photonics Society Distinguished Lecturer Award in 2014 and 2015. He was an elected member of the Society's Board of Governors for the term 2017–2019. He is currently serving as the Secretary-Treasurer for the IEEE Photonics Society for the term 2020–2022.

Yutaka Miyamoto (Member, IEEE) received the B.E. and M.E. degrees in electrical engineering from Waseda University, Tokyo, Japan, in 1986 and 1988, respectively, and the Dr.Eng. degree in electrical engineering from Tokyo University, Tokyo, in 2016.

He joined NTT Transmission Systems Laboratories, Yokosuka, Japan, in 1988, where he engaged in research and development on high-speed optical communications systems, including the 10-Gbit/s first terrestrial optical transmission system (FA-10G) using erbium-doped fiber amplifier (EDFA) inline repeaters. He was with NTT Electronics Technology Corporation, Atsugi, Japan, from 1995 to 1997, where he engaged in the planning and product development of high-speed optical modules at the data rate of 10 Gb/s and beyond. Since 1997, he has been with the NTT Network Innovation Labs, where he has contributed in the research and development of optical transport technologies based on 40-/100-/400-Gbit/s channel and beyond. He is currently an NTT Fellow and the Director of the Innovative Photonic Network Research Center, NTT Network Innovation Laboratories, where he has been investigating and promoting the future scalable optical transport network with the Pbit/s-class capacity based on innovative transport technologies, such as digital signal processing, space-division multiplexing, and cutting-edge integrated devices for photonic preprocessing.

Dr. Miyamoto is a Fellow of the Institute of Electronics, Information and Communication Engineers (IEICE).

David T. Neilson (Fellow, IEEE) received the B.Sc. and Ph.D. degrees in physics from Heriot-Watt University, Edinburgh, U.K., in 1990 and 1993, respectively. His doctoral thesis was on "Optical Nonlinearities and Switching in InGaAs Quantum Wells."

He is currently the Group Leader for Optical Transmission Research at Nokia Bell Labs, Murray Hill, NJ, USA, and a Bell Labs Fellow. The departments in the group conduct research into the next generation of terrestrial and undersea optical systems, including ultrahigh baud rates, modulation formats and coding, and the use of space-division multiplexing, for scaling system capacities. He joined Bell Labs in 1998, where he led research on optical switching systems and on optoelectronic integration. This includes MEMS and LCoS for wavelength-selective switches and optical cross-connects; InP optoelectronic growth and fabrication; and silicon photonics. From 1993 to 1996, he was a Postdoctoral Researcher working on free-space optical interconnect and switching systems with Heriot-Watt University. From 1996 to 1998, he was a Visiting Scientist with NEC Research, Princeton, NJ, USA, researching optical interconnects for high-performance computing systems. He has authored more than 200 publications, patents, and short courses, on both devices and systems in the field of optical interconnects and switching.

Dr. Neilson has served and chaired several IEEE-LEOS, OSA, and SPIE conference programs in the field of optical interconnects and switching.

Ioannis Tomkos (Fellow, IEEE) is currently a Professor of optical communications with the Department of Electrical and Computer Engineering, University of Patras, Patras, Greece. His research is focusing on optical networks and 5G networks. In the past, he held various academic and managerial positions, of increasing responsibility, at companies and academic institutions around the world. Over the past 20 years, he has managed teams that participated in industry research and development projects and in over 25 EU-funded industry–academia collaborative projects with a consortium-wide leading role (including being the Technical Manager of ten major projects with a total budget of over 50M€). For his research group, he has raised about 9.5M€ in funding, all as a Principal Investigator (PI) of his institution. His research activities resulted in over 650 coauthored scientific archival articles, with over 410 entries at IEEEXplore.

Prof. Tomkos has been elected as a Fellow of two major societies: the Institute of Engineering and Technology (IET) in 2010 and the Optical Society of America (OSA) in 2012.